POLYMER REVIEWS
https://doi.org/10.1080/15583724.2022.2132509

Taylor & Francis
Taylor & Francis Group

REVIEW

Hierarchical Design Strategies to Produce Internally Structured Nanofibers

Saptasree Bose[a], Victoria Padilla[a], Alexandra Salinas[a], Fariha Ahmad[a], Timothy P. Lodge[b,c], Christopher J. Ellison[c], and Karen Lozano[a]

[a]Department of Mechanical Engineering, University of Texas Rio Grande Valley, Edinburg, Texas, USA; [b]Department of Chemistry, University of Minnesota, Minneapolis, Minnesota, USA; [c]Department of Chemical Engineering & Materials Science, University of Minnesota, Minneapolis, Minnesota, USA

ABSTRACT

Nanofibers have attracted significant interest due to their unique properties such as high specific surface area, high aspect ratio, and spatial interconnectivity. Nanofibers can exhibit multifunctional properties and unique opportunities for promising applications in a wide variety of fields. Hierarchical design strategies are being used to prescribe the internal structure of nanofibers, such as core-sheath, concentric layers, particles distributed randomly or on a lattice, and co-continuous network phases. This review presents a comprehensive overview of design strategies being used to produce the next generation of nanofiber systems. It includes a description of nanofiber processing methods and their effects on the nano- and microstructure. Physico-chemical effects, such as self-assembly and phase separation, on the ultimate morphology of fibers made from designed emulsions, polymer blends, and block copolymers, are then described. This review concludes with perspectives on existing challenges and future directions for hierarchical design strategies to produce internally structured nanofibers.

ARTICLE HISTORY
Received 9 March 2022
Accepted 29 September 2022

KEYWORDS
Nanofibers; polymers; internally structured nanofibers; hierarchical design

1. Introduction

Nanomaterials are a promising and versatile class of materials with intriguing chemical and physical properties; typical examples are zero-dimensional nanoparticles or quantum dots, one-dimensional nanowires, nanorods, nanofibers, or two-dimensional nanosheets. Among these various classes, nanofibers (NFs) have emerged with a wide range of potential applications due to their small diameters, ranging from ten to hundreds of nanometers. NFs have unique properties that include high specific surface area, high aspect ratio, flexibility, spatial interconnectivity, and, most importantly, the ability to be formed into sophisticated macroscopic structures, such as 2D and 3D scaffolds with desired directional properties.[1–5] The architecture of scaffolds can enhance the repair or regeneration of various types of tissues (*e.g.*, nerve, skin, heart, blood vessel, and musculoskeletal system) and tissue interfaces.[6] The porous morphology of NF scaffolds is also useful for high-performance filtration media, artificial blood vessels, biochips,

CONTACT Karen Lozano karen.lozano@utrgv.edu Department of Mechanical Engineering, University of Texas Rio Grande Valley, Edinburg, TX 78539, USA

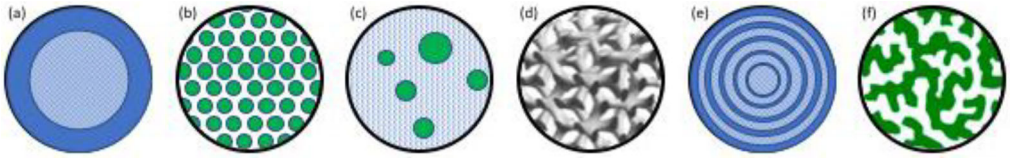

Figure 1. Schematic cross-section of internally structured NFs: (a) core-sheath, (b) ordered particles, (c) random particles, (d) bicontinuous gyroid, (e) concentric layers, and (f) bicontinuous microemulsion.

nano sensors, and composite materials. NFs can be synthesized from various building blocks including natural polymers, synthetic polymers, carbon-based materials, semiconducting materials, and composite materials. Triggered by the rapid progression within the various applications of NFs, significant efforts have been made to explore a wide variety of novel functional applications for energy generation and storage (e.g., flexible solar cells, fuel cells, batteries, and supercapacitors), optoelectronics, water treatment, healthcare, food packaging, and biological applications.[6,7]

To achieve next-generation NFs with greatly enhanced functionalities, it is highly desirable to design strategies to produce internally structured NFs (see Figure 1). Examples include core-sheath and concentric layers (a,e), particles distributed randomly or on a lattice (b,c), and co-continuous network phases (d,f). Layered structures permit the independent tuning of surface and bulk properties, as well as control over erosion and release of active agents, *e.g.,* therapeutics. Particle phases allow distribution of encapsulated ionic, optical, electronic, or catalytic functionalities. Co-continuous phases offer independent control over transport and mechanical properties, and templates for preparing porous NFs by selective etching or removal of one component. In general, combining internal fiber structures with the intrinsic structure of the non-woven mat (*e.g.,* mat density and fiber orientation) affords nanofiber systems that constitute robust and functional mesoscopic hierarchical 3D-network materials.

The ability to prescribe the internal organization of nanofibers opens up the opportunity to work with another level of hierarchical design, the bridge from nanoscale to macroscale. Developed nanofiber systems can be aligned and form strings which consists of multiple fibers twisted into a single yarn. Li, *et al.* have shown how bottom-up strategies can align cellulose nanofibers by assembling nanoscale fibrils into ordered macroscale materials.[8] Effective alignment of tunable cellulose nanofibers can be converted into the hierarchical structure of macroscale materials which may have different stiffness than the parent nanofibers. Zhang and Chang produced patterned fibers using a patterned fiber collector; they demonstrated the effect of electroconductive wire diameters on the fiber orientation.[9] Yan, *et al.* reported self-assembly of nanofibers into honeycomb-patterned nanofibrous structures (HNFSs) for three polymers, PAN, PEO and PVA.[10]

Several reviews have addressed the importance of polymer precursors and their influence on fiber production, properties and applications; reviews on theoretical simulations/modelling have focused on large-scale fiber production, research challenges, and future scientific regulations.[11–14] However, this work focuses on progress made in designing and controlling the internal structure of fine fibers. A variety of internal NF morphologies have been reported, such as those depicted in Figure 1. Some of these

structures have been achieved by simply combining polymer solutions and subsequently removing one component through post-processing procedures, or by exploring spontaneous self-assembly and surface-energy-driven processes fuzing NFs at crossover points through thermal treatment. The field of designing the next-generation NFs with increased functionality is vast. This review is organized as follows: first, an overview of NF fabrication methods; second, a general description of different types of internally structured NFs; third, a discussion of the methods and precursor systems that have been useful in engineering internal structures, while highlighting the most relevant examples; this review concludes with a summary that provides perspectives on existing challenges and future directions for hierarchical design strategies to produce internally structured NFs.

2. Overview of fabrication methods for nanofiber production

NFs at the laboratory scale are mostly produced through spinning (i.e., melt and solution blowing, electrospinning and forcespinning) and wet chemistry (i.e., template synthesis, phase separation, and self-assembly) methods.[12,15–35] For nanofiber production, electrospinning and forcespinning (FS) are so far the only methods with proven industrial yield. To manipulate, design, and optimize the internal structure of fibers, it is imperative to understand the NF production methods and how they influence ultimate NF geometry. In melt-blowing, a process widely adopted for industrial production of micron size fibers, fibers are produced by forcing a polymer melt through a fine orifice after which the melt is then drawn using a stream of hot air. Solution blowing is very similar, although it uses a polymer solution and therefore hot air is not necessarily needed. When the high-speed gas stream intrudes upon the melt or solution as it comes out of the spinneret, the force applied by the air converts the melt or solution extrudate into fibers, which are collected a few feet away from the orifice.[36–40] The web properties and fiber diameter are controlled by the polymer selection, viscosity, rate of polymer extrusion, temperature, and velocity of the applied air stream.[37,41] A wide variety of polymers have been used, such as polyethylene (PE), polypropylene (PP), poly(methyl methacrylate) (PMMA), poly(ethylene terephthalate) (PET), poly(butylene terephthalate) (PBT), polyamides, and polystyrene (PS). As for production of NFs, the high energy consumption and need for supersonic air speed could hinder melt blowing opportunities for large scale fiber production. Recent work has shown the influence of die design and operational parameters to increase production rate of submicron fibers.[42] Another approach to increase yield is to use polymer blends followed by subsequent removal of one component; using this multi-step approach, nanofiber mats with average diameters as small as 70 nm have been demonstrated.[43,44] In the case of melt-blowing, industrial scale production of fibers in the nanometer range has not been reported. Several lab scale studies have reported fibers as small as 500 nm, while industrial scale systems have fiber diameters of a few microns or greater. A recent study has described the use of melt blowing to control the internal structure of micron size fibers using a co-continuous binary polymer blend; an interpenetrating domain structure was obtained with control over domain sizes within the fibers to as small as 100 nm.[45] The above mentioned

strategies have fueled interest in further exploring the hierarchical design of NF structure through melt blowing techniques.

Electrospinning relies on the electrostatic repulsion between surface charges to continuously draw NFs from a viscoelastic fluid.[6,15,17,46–48] The setup is based on an electrohydrodynamic process and requires specific arrangements such as high voltage, a metal collector plate, a syringe pump, and a spinneret/hypodermic needle with a blunt tip/capillary cylinder designed with a metallic syringe. The power is supplied by a direct current (DC) or alternating current (AC).[6,17] Two electrodes are connected through the syringe and grounded through the collection plate. A small amount of a viscoelastic fluid is pumped out through the spinneret, producing a pendant droplet as a result of surface tension. Under an electric field, the electrostatic repulsion among the surface charges deforms the droplet into a Taylor cone; a charged jet is ejected, followed by the stretching and elongation into fine fibers,[6,49] which rapidly solidify under the action of a fiber whipping process. Finally, the solid fibers are deposited on the grounded collector. The fiber morphology, architecture, and diameter are mostly controlled by parameters related to the polymer solution, electric field strength, distance to the collector, and humidity of the environment.[6] Different types of electrospinning setups are typically used for NF production, such as single nozzle, multi-nozzle, and co-axial electrospinning.[5] Even though bulk production has been achieved, such as the process presented by Jirsak, *et al.*,[50] there remain challenges for commercial production. The need for materials with specific dielectric properties, inherent safety requirements, and expensive solvent recovery steps have been discussed as potential industrial production limitations.[12,51,52] The electrospinning process is capable of producing fiber membranes with small, highly homogeneous fibers with tight control over fiber diameter and mat density. Special types of collectors are also used to manipulate fiber deposition and develop different pore sizes depending on the ultimate application.[53–57]

Electrospinning has been the most popular method to produce nanofibers in the lab. On the industrial scale, many companies have launched systems based on multiple needles positioned in parallel, though the yield is still relatively low. El Marco was the first company to use a variation of the typical needle-based system. El Marco nanofiber production is based on a needle-less system (rotating drum), which can produce much higher yield and broaden the deposition area. In general, electrospinning systems (including industrial yield attempts), as reported by Omer *et al.*, can produce average fiber diameters as low as 80 nm.[58] Production of fibers using centrifugal force, known as the FS or rotary jet-spinning methods, has shown potential to overcome limitations observed in other methods while offering industrial scale fiber yields. NFs can be produced from polymeric solutions or molten polymers. The employed solvent does not require specific dielectric properties.[51,59] This technique was first introduced in 2009 as Forcespinning® by Fiberio Technology Co. (acquired by Clarcor Inc. in 2016, and Parker Hannifin in 2017). This technology was developed at the University of Texas Rio Grande Valley, with the initial patents filed by Lozano and Sarkar before being commercialized by FibeRio.[20,60–64]

In the FS process, fiber production begins with depositing the polymer solution or melt into a special spinneret that rotates the fluid until a critical angular velocity is reached and produces a jet that is then reduced in diameter as it expands outwards as a

spiral until collected either by vertical posts (lab scale) or deposited on a conveyor belt (industrial scale). Fiber formation variables such as intrinsic properties of the system (e.g., viscoelasticity and surface tension) and processing parameters (e.g., angular velocity, exit nozzle, and nozzle-collector distance) are carefully selected to obtain desired diameters from NFs to microfibers.[20,65] Yields as high as 50–100 $g \cdot h^{-1}$ have been reported at laboratory scales or as hundreds of meters per minute for continuous production of nonwoven fiber-based membranes in industrial scale systems.[51,59,66–68] Forcespinning has shown the highest industrial yield, and the average fiber diameters at this scale compare well with electrospinning. Solution-based systems have led to average fiber diameters as low as 80 nm while fibers produced from polymeric melts have shown average fiber diameters in the low 400 nm (i.e., polypropylene, as reported by the Lozano team).[69]

As for wet chemistry methods, template synthesis uses a nanoporous membrane template to fabricate NFs.[15,70] Generally, a porous metal oxide membrane containing a large number of holes with a narrow size distribution is used as the template. Tao *et al.* and Pender *et al.* used the template synthesis method to fabricate biodegradable, eco-friendly PCL (poly(ε-caprolactone)) and aligned boron-carbide NFs, respectively.[71,72] In this method, when a polymer solution is pushed through the nanopores, short NFs are produced, and their diameters depend solely on the template pore size.

In self-assembly, a bottom-up fabrication method, where atoms, molecules, or nanoscale building blocks spontaneously arrange themselves into ordered structures using intermolecular interactions, NFs are formed from suitable synthetic amphiphilic molecules in aqueous or non-aqueous media.[73] An example of this process is the assembly of NFs from small peptide amphiphiles formed due to end-point protein aggregation.[74] This process is considered a wet-chemistry method and the fiber yield is generally extremely low for industrial applications.[61,75] The processing parameters to be considered are mostly related to the intrinsic chemistry of the system (i.e., pH, ionic strength), temperature, assembling rate, chosen solutions and substrates.[74]

The method of phase separation is typically based on the extraction of a solvent-rich phase from the solution due to a physical incompatibility produced by a temperature change.[76] This method allows for the production of porous NFs that could be useful in drug delivery applications or as templates for the formation of inorganic fibers. Producing NFs through the phase separation method involves four major steps: (1) dissolution of a polymer in a solvent at room temperature or elevated temperature until a homogeneous solution is obtained; (2) gelation, the prime step for the formation of a 3D network by chemical or physical cross-linking; (3) extraction of the solvent from the gel; and (4) freeze-drying, which finally delivers the porous nanofibrous mat.[76] The phase separation process is time-consuming, precludes the formation of continuous fibers, and restricts polymeric choices.[61,74,75] Thermally-induced phase separation (TIPS) is a common method used to develop well-defined porous structures by separation of polymer solutions based on thermodynamic parameters. TIPS uses temperature change to trigger de-mixing of an homogeneous polymer solution, resulting in the formation of a multi-phase structure which allows control of fiber porosity.[15] Dual-phase TIPS has been used to produce nanofibrous poly(L − lactide) scaffold as well as chitosan nanofiber decorated micropore channels.[77]

Table 1. Comparison of advantages and disadvantages of different processes to make fibers.

Method	Industrial suitability	Advantages	Disadvantages
Melt-blown	High	Long fine fibers, high productivity, no solvent required	Only works with limited number of polymers, thermal degradation of polymers, fiber uniformity, not suitable for industrial scale of nano or submicron scale fibers
Electrospinning	Medium	Long continuous NFs with uniform diameters; wide range of fiber diameter; needleless systems have high throughput	Need for high electric fields, safety requirements, fire hazard, need for special dielectric properties (which usually require costly, toxic organic solvents). Mostly solution-based process, adding cost of solvent recovery and other safety issues
Forcespinning	High	Wide range of polymeric systems, highest yield, suitable for melt and solution spinning, and does not require high voltage or specific dielectric parameters	Production of fibers from melt results in larger diameter when compared to solution-based systems

Table 1 presents a comparison of advantages and disadvantages of the available methods to produce fine fibers. In summary, electrospinning and forcespinning are the methods with proven industrial potential. The major drawbacks of the electrospinning process involve (i) the need for certain dielectric properties (therefore use of costly and/or toxic organic solvents), (ii) high electric fields (therefore higher energy input), (iii) low yields. As for centrifugal spinning methods, these have much higher production rates, no need for electric fields (therefore no constraints on dielectric parameters, which broadens the spectrum of usable materials).[20] In fact, it is considered to be a green technology (this technology placed in the top 100 out of over 6,000 nominated technologies).[78]

3. Internally structured nanofiber architectures

Although various fiber processing techniques have been developed, the correlation of these methods with prescribing internal structure of NFs has not yet been extensively elucidated, except for some studies that have used electrospinning to produce mesoporous, core-sheath, and hollow fibers.[6,17,39,46,79–83] NFs are generally classified based on their (1) chemical composition, e.g., polymeric, carbon, ceramic, metallic, metal oxide, or hybrid-based content; (2) size, e.g., fiber diameter, pore size, thickness of the mat, and fiber length; and (3) morphology (as previously shown in Figure 1), core-sheath and concentric layer structures (Figure 1a,e), particles distributed randomly or on a lattice (Figure 1b,c), and co-continuous network phases (Figure 1d,f).

Core-sheath NFs are a special type of internally structured NF, often made from a bicomponent system, with one component as the inner capillary (core) and the other as the outer capillary (sheath), as shown in Figure 2. In comparison to monolithic NFs, core-sheath structures have proven to be beneficial for several applications, particularly in biomedicine (e.g., in controlled drug release and stabilization of protein structures).[85–87] Different processes and combinations of materials have been used to

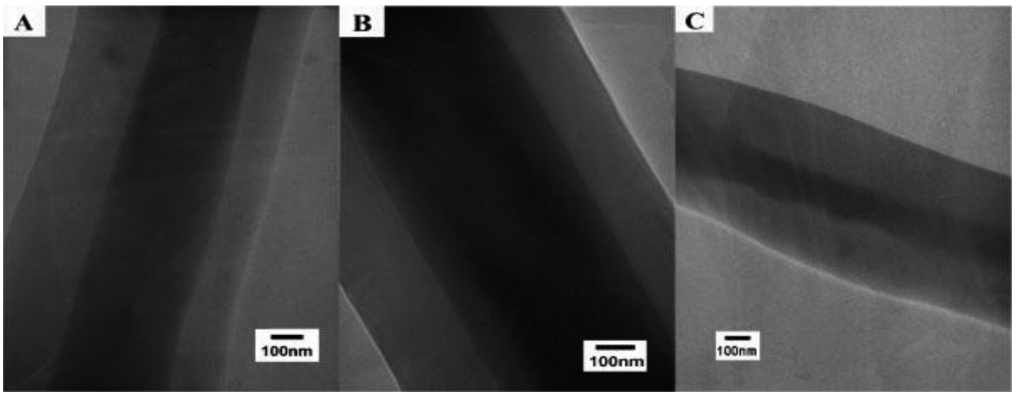

Figure 2. TEM images of core-sheath NFs using poly(ethylene oxide) (PEO) as the core and amphiphilic poly(ethylene glycol)-poly(L-lactide) (PEGPLA) diblock copolymer as the sheath using three polymer-in-water concentrations to form the core: (A) 45 mg/mL, (B) 58.5 mg/mL, and (C) 34.5 mg/mL.[84] Reprinted from Xu *et al.*,[84] Copyright (2006), with permission from Wiley.

develop core-sheath structures. For example, Sahoo *et al.*[88] prepared electrospun NFs of poly(D,L-lactide-*co*-glycolide) (PLGA) loaded with fibroblast growth factor (bFGF) using two techniques: blending electrospinning (one needle) and co-axial electrospinning (two concentric needles). Similarly, Jia *et al.*[89] prepared core-sheath fibers by coaxial electrospinning, where PLGA was used as the outer shell polymer and dextran (DEX) as the core material. Vascular endothelial growth factor (VEGF) was encapsulated within the fibers and its effectiveness in vascular tissue engineering applications was analyzed. Core-sheath NFs have been widely reported using a coaxial electrospinning processes, using double-capillary spinnerets or emulsion-based systems, where two polymers are present in two immiscible solvents. Still, the development of core-sheath fibers using the electrospinning process remains a challenge, particularly in the control of the thickness of the inner and outer layers and in the position of the core, which often presents itself on or near the surface of the fiber.[90,91]

Triple-layer nanofiber scaffolds from PLGA/collagen/PLGA were fabricated by Arabpour *et al.* using electrospinning for applications in corneal tissue engineering.[92] The developed layered scaffold was cross-linked to retard degradation. The effect of polymer concentration, applied voltage, flow rate, and rotational speed of the collector system on the development of the layered structure was evaluated. Han, *et al.* used coaxial electrospinning to develop concentric layers for drug delivery applications.[93] They developed bis-chloroethyl-nitrosourea impregnated into multi-layer fiber membranes with a core/sheath ratio of 20:80, where the polyanhydride poly-(1,3 bis[p-carboxyphenoxy] propane-*co*-sebacic acid) and poly(ε-caprolactone) (PCL) were the core and sheath, respectively.

In the development of core-sheath fiber systems, block copolymers (BCP) have been utilized either as the core or the sheath.[94,95] Fibers formed through self-assembly processes using BCP, such as those shown in Figure 3, have promising potential applications, particularly in tissue engineering and drug delivery.[92,93,97] Ma *et al.* used a two-fluid coaxial electrospinning technique to obtain core-sheath fibers where BCP was confined as the cylindrical core within a protective polymer sheath.[96] In their work,

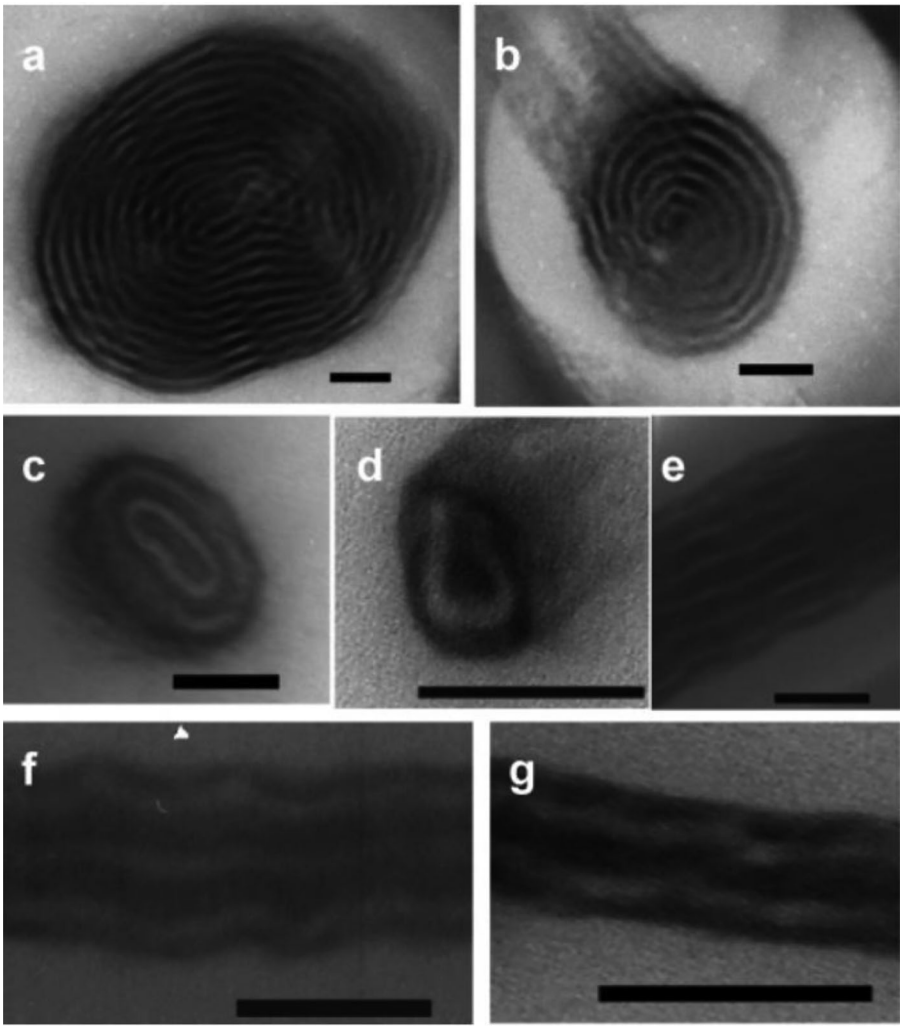

Figure 3. TEM images of the SIS BCP in the fiber cores of different diameters after annealing. Scale bar: 100 nm: (a-d) axial views; (e-g) longitudinal views.[96] Reprinted from Ma *et al.*,[96] Copyright (2006), with permission from American Chemical Society.

poly(methylmethacrylate-*co*-methacrylic acid) random copolymer was used as the sheath system with cores from two different symmetric triblock copolymers comprised of polystyrene and polyisoprene (SIS) that formed lamellar or spherical morphologies. In their work, the developed fibers had diameters ranging from 300 to 800 nm while the core diameters varied from 50 to 500 nm. To facilitate long-range order and improve the internal structure, fibers were annealed in a vacuum oven at 140 °C for 10 days.

The structure of fibers can also be altered by selectively prescribing porosity. Fibrous materials possess intrinsically high specific surface area, which can be further enhanced by introducing porosity on the fiber surface or within the fibers (internal pores). Different strategies have been employed to achieve mesoporous nano/microfibers with enhanced pore uniformity and surface area. Studies have shown how the ultimate fiber properties can be significantly altered by introducing porosity within the fibrous

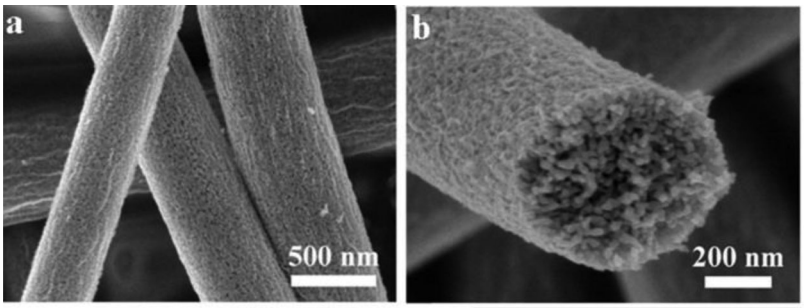

Figure 4. SEM images of mesoporous TiO_2 NFs, to depict surface morphology (a) and fiber core (b).[105] Reprinted from Hou *et al.* (b),[105] Copyright (2014), with permission from American Chemical Society.

membrane while maintaining micro/nano-structural features. Unique qualities of organic and inorganic nanoporous fibers have shown their improved performance in a variety of fields, such as drug delivery, tissue engineering, photocatalysis, sensors, and lithium-ion batteries.[98–102] Nanoporous 1D structures are appealing in electrochemical applications as the void spaces can increase charge capacity and accommodate volume changes experienced during charge/discharge processes. Zhang *et al.*, Kim *et al.*, and Lin *et al.* achieved different types of NFs systems where internal pore structures, including the pore size and size distribution, can be adjusted by tuning different process parameters.[102–104]

A facile foaming-assisted electrospinning technique to create mesoporous titanium dioxide (TiO_2) NFs with uniform porosity (average pore diameter $\sim$ 16 nm) was reported by Hou *et al.* Through electrospinning, they developed precursor fibers using polyvinylpyrrolidone, tetrabutyl titanate, and diisopropyl azodiformate as the foaming agent; these precursor fibers were later calcined at 550 °C (Figure 4).[105]

Altering the surfaces of NFs has proven an effective method to enhance their multifunctionality, and such approaches can leverage and be amplified by prescribing the internal structure. The higher surface area in lamellar type morphologies increases the abundance of electrochemically active sites. Elishav *et al.* have shown that ceramic fibers with a lamellar type structure have potential as Li-ion battery anode materials.[106] They have demonstrated how altering the ratio of precursor fiber materials (acetylacetonate/PVP) has an interesting effect on the ultimate structure, morphology, and directional property of the lamellar type structure on the surface of the ceramic based NFs (Figure 5). Ma *et al.* also exemplified how fiber morphology can be controlled even in core-sheath systems by tuning the interactions between the polymer blocks and sheath components. They created continuous core-sheath NFs with long-range ordered internal structures through self-assembly of BCPs where poly(styrene)-*b*-poly(dimethylsiloxane) (PS-*b*-PDMS) block copolymer acted as the core and a poly(methacrylic acid) (PMAA) homopolymer as the sheath. After a long annealing process (10 days), a concentric lamellar structure was formed within the fiber.[107]

Network structures, such as the double gyroid, are promising architectures for a variety of applications. The interfacial topology belongs to the triply periodic minimal surface (TPMS) family.[108] TPMS systems have zero mean curvature, and divide space into continuous nanophases, making it possible to create composite materials with

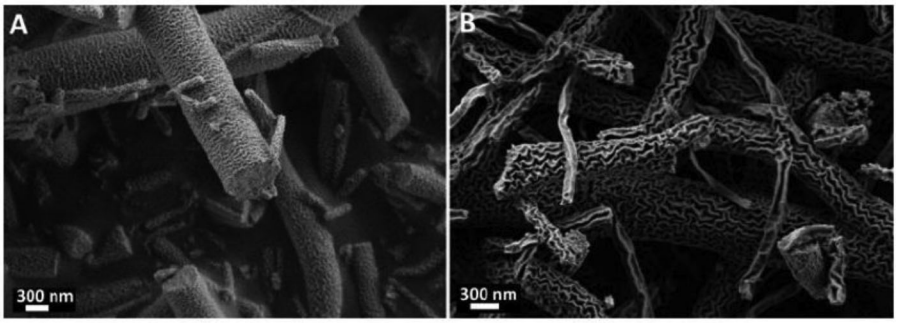

Figure 5. Nanofibers with different acetylacetonate (acac)/PVP ratios after heating to 220 °C. (A) 1.0, and (B) 1.2.[106] Reprinted from Elishav *et al.*,[106] Copyright (2020), with permission from Royal Society of Chemistry.

continuous and interconnected reinforcements.[109] There are various TPMS structures, such as primitive, double gyroid, and double diamond, which exhibit different characteristics including mechanical properties like compressive strength, fracture toughness, and elastic modulus; the double gyroid is the most prevalent TPMS structure. Network structures have shown potential in the biomedical field due to their high porosity and effectiveness for cell growth and migration. Promising applications have also been envisioned in filtration, pharmaceuticals, and environmental remediation.[110] Despite this, fibers with the gyroid morphology have not been widely explored. The few reported studies have focused on the use of BCPs to form fibers via electrospinning.[111] For example, as noted above Ma *et al.* have shown that gyroid-forming PS-*b*-PDMS block copolymers can also be used as a core component with a PMAA sheath, resulting in fibers with various gyroid structures produced via co-axial electrospinning followed by thermal annealing.[112]

4. Physico-chemical methods used to prescribe the internal structure of NFs

Self-assembly during fiber production is a promising route to produce and control the internal structure of NFs through the interplay of thermodynamically-driven and kinetically-limited processes.[113] Self-assembly and phase separation effects have an important role on the ultimate morphology of fibers made from emulsions, polymer blends, and block copolymer-based systems that when combined with selected processing methods, the ultimate fiber architectures present a multitude of possible combinations.[114] Bicontinuous or discontinuous phases with different morphologies and properties can be achieved by tuning the molecular weight and composition of the constituents, and the selected processing method. While self-assembly and phase separation processes are relatively well-understood at equilibrium, at least three factors present in NFs may influence the selection of the ultimate nanostructure: (*i*) *preferential surface wetting*, which can drive adoption of different structures or gradients in structure; (*ii*) *confinement effects*, which can modulate both the structure and the physical properties (*e.g.*, T_g and T_m); and (*iii*) processing induced *deformation rates* which can guide the nucleation and growth of a specific nanostructure, possibly with preferential orientation. The following section reviews the physico-chemical dependent systems used to prescribe NF internal

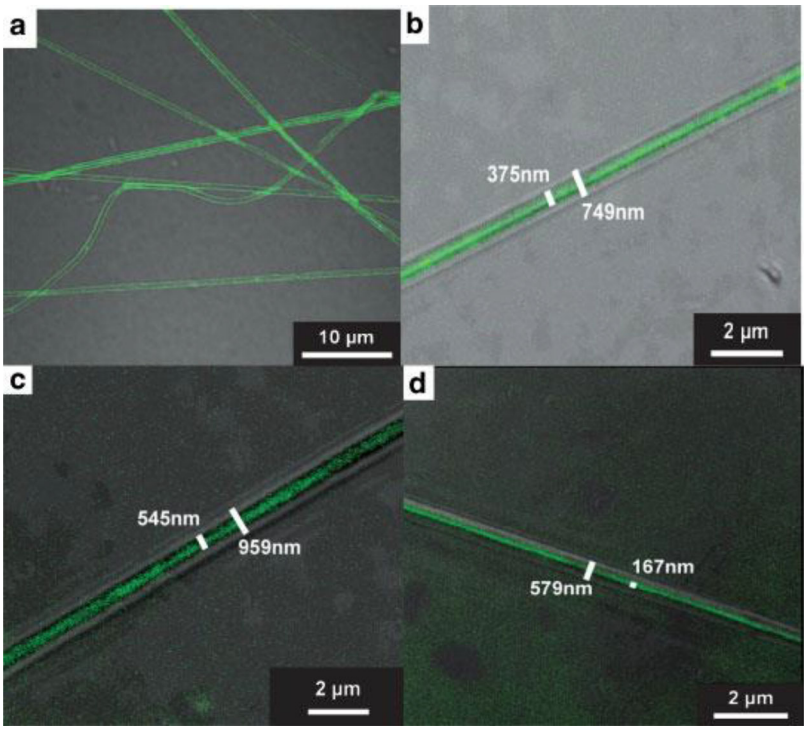

Figure 6. Confocal laser scanning microscope (CLSM) images of core-sheath structured NFs prepared from W/O emulsions. The concentrations of the core polymer, PEO-FITC, in the aqueous phase were (a,b) 45 mg/mL (c) 58.5 mg/mL, and (d) 34.5 mg/mL, respectively. It should be noted that (a) is an overview of the composite NFs, and (b) is a segment of the nanofiber.[84] Reprinted from Xu *et al.*,[84] Copyright (2006), with permission from Wiley.

structure, which may be broadly classified as emulsion, block copolymer, and blend-based systems.

4.1. Fibers made from emulsion-based systems

An emulsion is a mixture of two or more immiscible liquids, one of which is typically distributed as small droplets throughout the other.[115] Emulsions can be classified based on the spatial organization: oil droplets dispersed in water is termed an oil-in-water (O/W) emulsion, and water droplets dispersed in oil is referred to as a water-in-oil (W/O) emulsion.[115,116] Conventional macroemulsion systems are kinetically stable but thermodynamically unstable; several mechanisms (*e.g.*, gravitational separation, flocculation, creaming, coalescence, and Ostwald ripening) can lead to macroscopic phase separation over time. To produce a long-lived emulsion of droplets, it is necessary to add a surfactant to act as a barrier between phases, increasing the emulsion stability. Surfactants can contain different chemical entities which may have an effect on the ultimate microstructure of a fiber system.[117] A microemulsion is an example of a high-surfactant-content system that is thermodynamically stable; it can exist in micellar (W/O or O/W) and bicontinuous structures.[118] A Pickering emulsion is stabilized by solid particulates as surfactants. Particles, such as polymer micelles, latex particles,

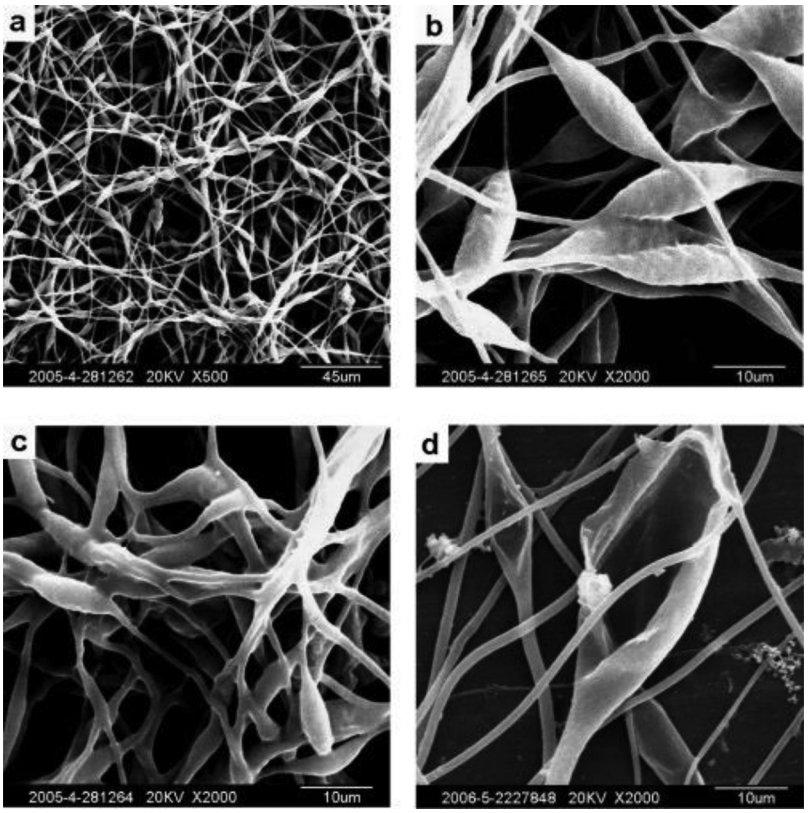

Figure 7. The morphology of fibers obtained via electrospinning of the emulsion-based system composed of Ca-alginate and PLLA (applied voltage in electrospinning: 20 kV). (a) Fibers before release test, 500× magnification; (b) fibers before release test, 2000× magnification; (c) fibers which were immersed in 0.9% NaCl water solution for 30 days; (d) fibers which were immersed in PBS for 6 days.[126] Reprinted from Qi *et al.*,[126] Copyright (2013), with permission from American Chemical Society.

inorganic particles, proteins, and even bacterial cellulose nanocrystals have been used for stabilization in Pickering emulsions.[119–122] This type of emulsion has found wide use in food, cosmetics, and pharmaceutical fields, especially where traditional surfactants are not suitable due to their health hazards.[119] Recently, graphene oxides (GO) have found attractive applications as Pickering agents due to their unique structure, amphiphilic nature, and potential use in the large-scale production of bio-compatible graphene-based materials.[120–122]

NFs from emulsion-based systems have been developed primarily using electrospinning.[123,124] Emulsion precursors are attractive in fiber-making systems since a single nozzle configuration can be used to create bilayer or multilayer structures, circumventing challenges that appear in coaxial systems. Xu *et al.*[84] have employed a unique method to fabricate uniform core-sheath NFs by using W/O emulsion electrospinning. They used a poly(ethylene oxide) (PEO) solution as the aqueous phase to design the core of the fiber, and a chloroform solution of an amphiphilic poly(ethylene oxide)-poly(L-lactide) (PEO-*b*-PLA) diblock copolymer as the oil phase to develop the sheath (Figure 6). The PEO in the core was labeled with fluorescein isothiocyanate (FITC) for

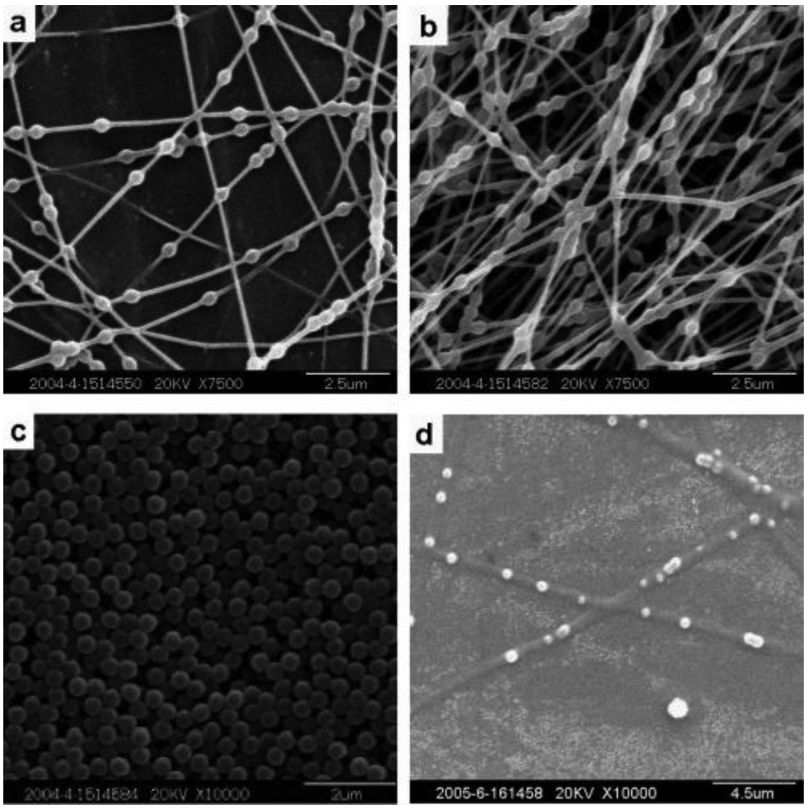

Figure 8. SEM micrographs: (a) electrospun fibers by emulsion (1 g PVA dissolved in 9 mL water and 1 mL original emulsion); (b) electrospun fibers by emulsion (1 g PVA dissolved in 8 mL water and 2 mL original emulsion); (c) PS microbeads in original emulsion; (d) composite fibers after solvent etching.[126] Reprinted from Qi *et al.*,[126] Copyright (2013), with permission from American Chemical Society.

identification. It was noted that fiber size and diameter can be effectively altered without the use of concentric needles, just by tuning the emulsion composition and the emulsification parameters. To elucidate the emulsion process in achieving different fiber (core and sheath) diameters, the team changed processing parameters, such as aqueous polymer concentration, volume fraction of aqueous and oil phases, and the rate of rotation of the homogenizer during the electrospinning process. The results of these changes were observed on the average droplet size and the outer and inner diameters of the core-sheath fibers ranged from $750-1500$ nm and $375-900$ nm, respectively. The electric field also contributed to the reorganization of the two immiscible phases; as droplets undergo coalescence, the core formation is based on a dielectrophoresis phenomenon where a force exerted on a dielectric particle promotes droplet deformation into an elliptical shape, ultimately becoming the core of the fiber.[125]

The use of emulsion precursor systems has also proven effective to produce beads and beads-on-string structures. In this case, the developed beads contain a dissimilar material, which contains an active ingredient and is encapsulated within a shell system.[126] Qi *et al.* use an aqueous phase consisting of droplets of an alginate-water

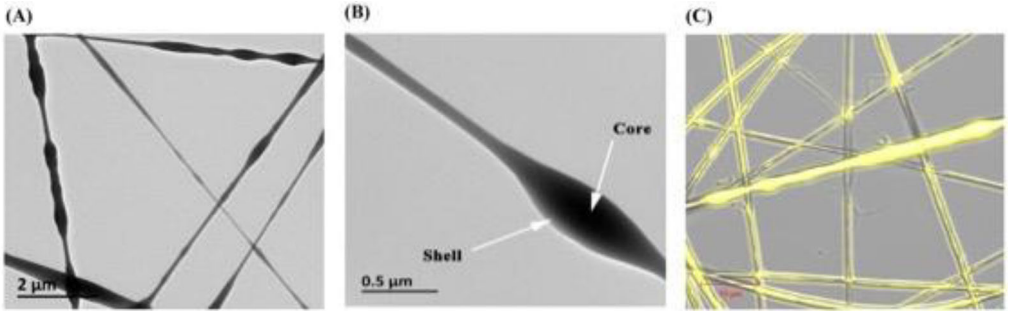

Figure 9. (a) and (b) TEM images, (c) confocal laser scanning microscopy images of the core – shell NFs by emulsion electrospinning[128] Reprinted from Zhang *et al.*,[128] Copyright (2018), with permission from American Chemical Society.

solution under a continuous oil phase consisting of the surfactant AOT (sodium bis(2-ethylhexyl) sulfosuccinate) and dichloromethane to encapsulate the alginate as beads within the continuous fiber system. Calcium chloride was added to this emulsion to serve as a cross-linking agent. PLLA was added to the external phase of the emulsion before electrospinning to undergo a dissolution process. When the emulsion was electrospun into fibers, the encapsulation of the calcium alginate within the PLLA produced beads-on-string fiber structures (Figure 7). The average diameter of these fibers and beads ranged from 1 – 3 microns and from 5 – 9 microns, respectively.

Similarly, the same group has reported on the beads-on-string fiber structure made from preformed polystyrene (PS) beads and polyvinyl alcohol (PVA) based systems.[126] They found that by varying the volumetric fraction of PS beads to PVA in the emulsions, the distance between adjacent beads within the fibers was altered proportionally (Figure 8).

Fibers fabricated through electrospinning emulsions of vascular endothelial growth factor (VEGF) along with protective agents (dextran (DEX) or bovine serum albumin (BSA))-loaded poly(lactide-*co*-caprolactone) (PLCL)) were reported by Tian *et al.*[127] These fibers were studied as potential systems for cardiac tissue regeneration, given the controlled release of VEGF. Emulsions for PLCL–VEGF–BSA and PLCL–VEGF–DEX were prepared by using VEGF in aqueous BSA or dextran solutions (water phase) and PLCL with span-80 chloroform (oil phase). Zhang *et al.*[128] prepared core – shell NFs by electrospinning gel-like corn oil emulsions, and gelatin was used as the stabilizer. They investigated how oil and water concentrations changed the internal structure and diameter of the fibers. Increasing oil volume fractions ranging from 0 to 0.6 led to an increase in the average diameter by increasing the viscosity of solution. Figure 9 shows the successful formation of corn-oil-in-water emulsion NFs. The corn oil was stained with Nile red to confirm its distribution within the core of the NF (Figure 9(c)).

To avoid the complexity and to increase the biocompatibility of fibers produced from emulsion electrospinning, researchers have developed stable emulsions without the use of surfactants. Li *et al.* produced core-shell fibers through the development of an emulsion comprised of two systems, a solution of PCL in a mixture of two solvents dichloromethane/hexafluoroisopropanol (DCM/HFIP) to be developed into the sheath of the

fiber, and a solution of silk fibroin (SF) in HFIP to form the core of the fiber.[129] The average diameter of NFs decreased upon increasing the concentration of SF in the two-phase system. This observation was explained on the basis of the conductivity of the emulsion. HFIP has high dielectric constant and electrical conductivity and SF is an amphiprotic macromolecular electrolyte, the conductivity of the emulsion increases and the HFIP solvent is completely evaporated upon fiber formation, leading to tighter control in fiber diameter.[130–132] Similarly, Camerlo *et al.* fabricated core-shell fibers via emulsion electrospinning using a stable surfactant-free limonene/PVA system.[133]

As mentioned, surfactants have been found to promote tuning of the internal structure/morphology of nano/microfibers produced from emulsion-based systems.[134] Studies have revealed that the type of surfactant and its concentration have a strong influence on the fibers and the fiber mat morphology. Hu *et al.* present examples depicting the role of surfactants on fiber characteristics; they investigated how the morphological, chemical, and mechanical properties of electrospun emulsions based on PCL/BSA were influenced by the nature of the surfactants, such as nonionic (Span80, Pluronic F108), anionic (sodium dodecyl sulfate (SDS)), and cationic surfactants (benzyltriethylammonium chloride (TEBAC)).[117] They observed that at a low concentration of Span80 (0.5%) and F108 (0.4%), fibers were formed with spindle-like beads, resulting in non-uniform fiber morphologies. Upon increasing concentration of Span 80 (1%) and F108 (0.5%), fibers showed cylindrical shapes with lower degrees of entanglement and smaller fiber diameters. On the other hand, TEBAC produced branched, bimodal, non-uniform fibers, and diameters changed from $\sim 190 - 250$ nm with increasing concentration of TEBAC. In the case of SDS, the emulsion produced smooth and uniform NFs with diameters ranging from $\sim$170 nm (lower concentration) to $\sim$260 nm (higher concentration). The authors proposed that an ionic surfactant produces a greater charge density in the emulsion jet, increasing the repulsion force that elongates the fiber toward the collector, thereby explaining the smaller diameter found with TEBAC and SDS. Wang *et al.* also reported morphological changes under the influence of SDS and Span80 on emulsion-electrospun core-shell fibers.[135] They used deionized water or phosphate buffer saline as the water phase and a PLGA solution as the oil phase to produce emulsion based nanofibers. Their investigations showed that using minimum amount of hydrophilic (SDS) or hydrophobic (span80) surfactant during emulsion preparation has significant influence on the core-shell structure of emulsion based electrospun nanofibers. Sanders *et al.* explained that in the electrospinning of emulsions, two types of Rayleigh instabilities occur. A type I capillary instability is produced when the viscoelastic force in the jet is not enough to form a continuous phase resulting in bead formation with encapsulated water-phase droplets. Type II relates to the core-shell formation and the interfacial tension between two emulsion phases play an important role; under this instability the internal phase core breaks up into smaller droplets.[136] Wang *et al.* showed the role of type II as the Span 80 reduced the interfacial tension and produced an elastic interfacial film, promoting a better defined core compared to the one formed by the SDS surfactant. The effect of SDS on reducing the interfacial tension was less, resulting in additional breakup of water-phase droplets.[135]

Most studies on fiber formation from emulsion-based systems have used the electrospinning method. Buzgo *et al.*[59] were the first to describe the development of core/

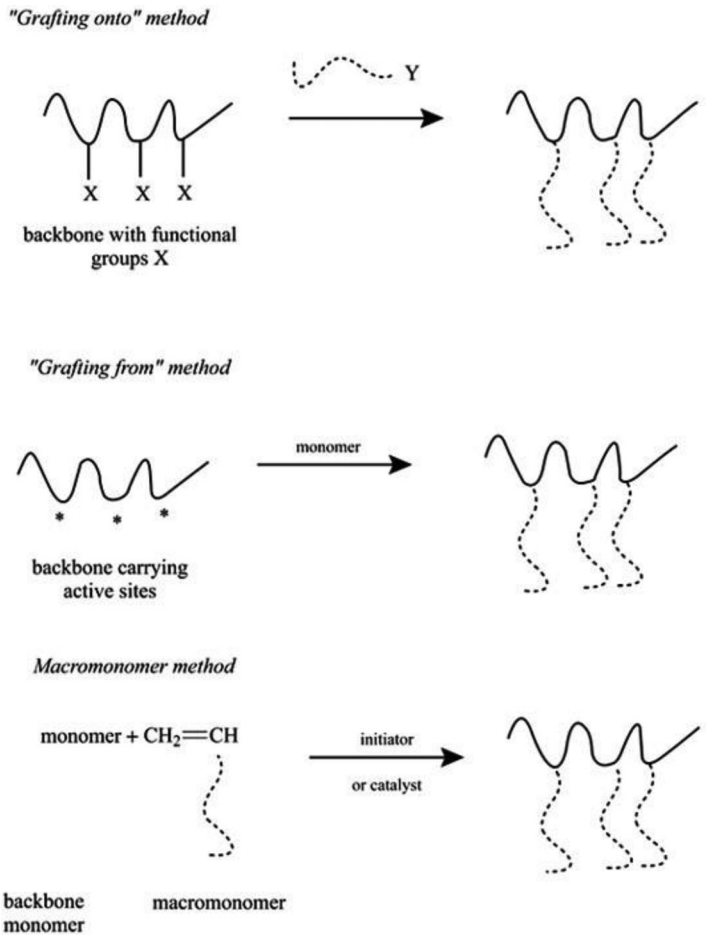

Figure 10. Three general methods of synthesis of randomly branched graft copolymers. (Top: "Grafting to" method. Middle: "Grafting from" method. Bottom: "Macromonomer method," "Grafting through" method.)[142] Reprinted from Hadjichristidis *et al.*,[142] Copyright (2010), with permission from Wiley.

sheath NFs from emulsion-based systems using centrifugal spinning. Fibers were produced from a water-in-oil (W/O) emulsion, where PCL dissolved in chloroform was used as the continuous phase or shell and Pluronic F-68 dissolved in ethanol served as the dispersed phase or core material. Microfibers with average diameters of $2.7 \pm 1.5\,\mu m$ and NFs with average diameters of $340 \pm 90\,nm$ were developed. The use of centrifugal spinning processes to produce fibers from emulsion-based systems remains an attractive area to be explored.

4.2. Fibers made from block-copolymer systems

Block polymers consist of two or more polymers with different properties that are covalently bonded. Diblock copolymers use two different polymer blocks, A and B, within the same chain, while triblock copolymers can consist of three polymer blocks that alternate, as in ABA or BAB. A segmented block copolymer consists of multiple small

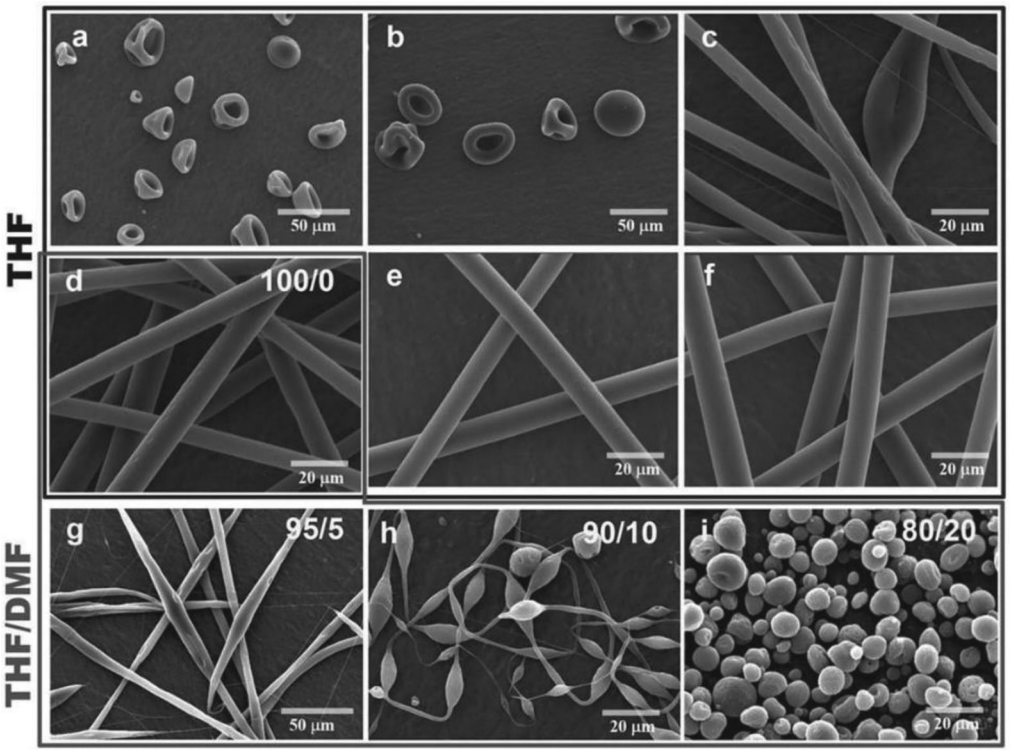

Figure 11. SEM images of electrosprayed beads (a,b) and electrospun fibers (c–f) of SEBS from neat THF solutions at varying polymer concentrations (8, 10, 12, 14, 16, and 18 wt% for (a)–(f), respectively). SEM images (d,g–i) show the effect of solvent composition (THF/DMF) on the morphology of electrically processed SEBS solutions at 14 wt% (THF/DMF = 100/0, 95/5, 90/10, and 80/20, for (d), (g), (h), and (i), respectively). SEBS: Polystyrene- b -poly(ethylene butylene)- b -polystyrene.[144] Reprinted from Wang *et al.*,[144] Copyright (2015), with permission from Wiley.

polymer blocks that alternate. Tapered block copolymers consist of having one side of the chain predominantly one polymer and the other side of the chain predominantly the other, with an intermediate zone of statistical copolymer with systematically varying composition.[137] Amphiphilic block copolymers contain at least one hydrophobic block and one hydrophilic block; these are typically used for the formation of micelles in aqueous solution.[138] The use of block copolymers to prescribe the internal structure of NFs is appealing for at least two reasons. One is the ability to produce a variety of interesting self-assembled nanostructures, and the second is the possibility to selectively remove one block, leaving a nanoporous material.[139]

The architecture of a block copolymer can increase in complexity, which can also result in detailed changes in the internal structure of NFs. Graft copolymers are among these complex structures, where one polymer serves as the backbone, while the other is covalently attached as branches or grafts. The structure of graft copolymers can vary with graft dispersity, graft length, and backbone length.[140,141] There are three major general graft polymerization methods: (1) "grafting-to," (2) "grafting from," and (3) "grafting through," which are used to yield grafted copolymers. These three methods are illustrated in Figure 10.[142]

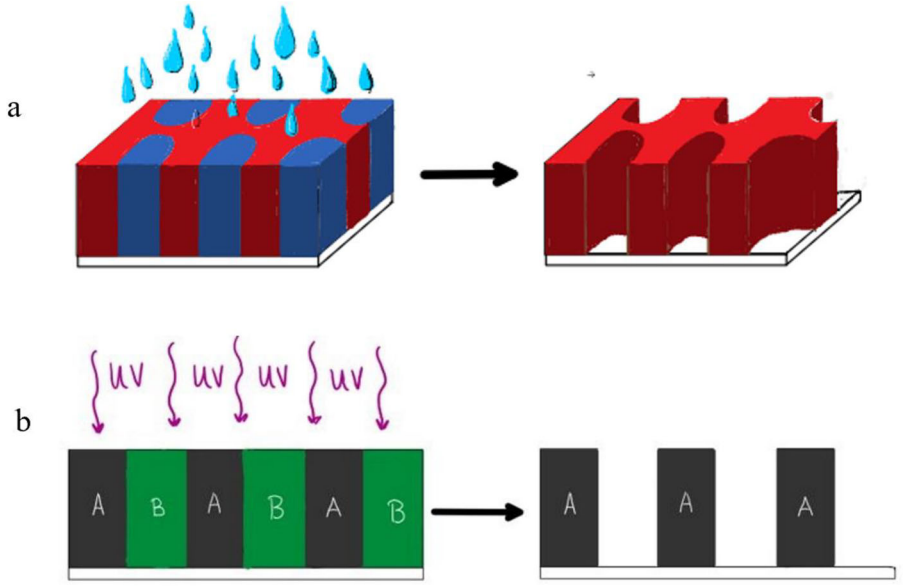

Figure 12. Illustrations of Chemical Degradation and UV degradation. Top a: Selective removal of blue polymer to result in the red polymer matrix. Bottom b: Selective removal of Polymer B through UV radiation degradation.[139]

To date, few studies have utilized block/grafted copolymers to form NFs with internal structures. As noted above, Ma *et al.* used a coaxial electrospinning process to prepare continuous concentric lamellar NFs using PS-PDMS as the core and PMAA as the shell. The confinement and annealing of the PS-PDMS block copolymer within the PMAA shell yielded a concentric lamellar structure. Furthermore, selective removal processes were performed to analyze the internal structure of the fiber.[107] Zhai *et al.* electrospun core-shell NFs through a single spinneret using PVA as the shell and PEO-*b*-poly(*p*-dioxanone) (PE-*b*-PPDO) as the core. The copolymer assembled into a lamellar structure as it was incorporated within the PVA, which promoted the ordered, well-defined alignment of the copolymer within the PVA shell.[143] In 2015, Wang *et al.* reported fibers dispersed with beads by utilizing a self-assembling PS-*b*-poly(ethylene butylene)-*b*-PS (SEBS) triblock copolymer in a selective solvent. The SEBS was dissolved within a co-solvent consisting of tetrahydrofuran (THF), appropriate for solvent for both blocks, and dimethylformamide (DMF), which is selective toward polystyrene. Alterations of the co-solvent ratio of THF to DMF caused morphological changes to the fibers, increasing concentration of DMF within the co-solvent solution generated a beaded morphology (Figure 11). This was attributed to the reduction of the copolymer chain entanglement as the copolymer experienced microphase separation.[144]

An attractive aspect of block polymer nanostructures is the possibility of the selective removal of one block, leaving a nanostructured porous material. The most commonly utilized methods to remove polymer blocks are chemical degradation, thermal/UV degradation, ozonolysis, and hydrolysis.[139] In selective removal through chemical degradation, a reactive polymer is dissolved/etched, which would leave the nonreactive

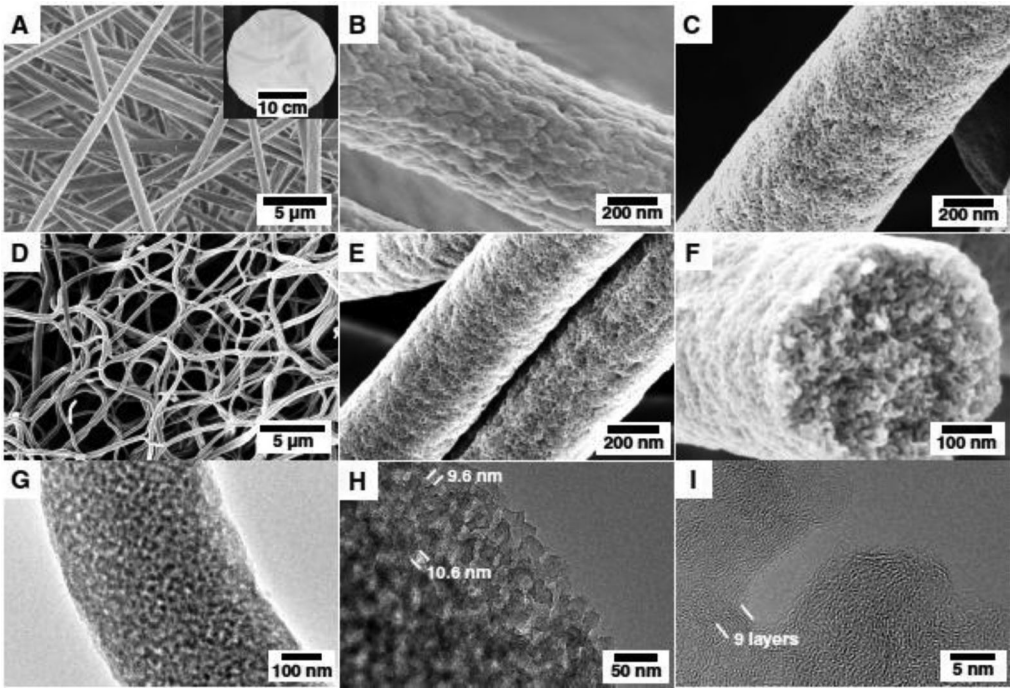

Figure 13. Microstructures of PCFs. SEM images of PAN-b-PMMA fibers (A and B) after electrospinning, (C) after oxidation and self-assembly at 280 °C in air, and (D to F) after pyrolysis at 800 °C in N2. Inset: A digital photograph of a piece of as-spun polymer fiber mat. (C) The bright and dark domains are PAN and PMMA, respectively. The good contrast between PAN and PMMA in the SEM image is due to the partial degradation of PMMA in air. (E and F) High-magnification SEM images of uniformly distributed mesopores in PAN-b-PMMA-CFs. (G and H) TEM images of mesopores in a PAN-b-PMMA-CF. (I) High-resolution TEM image of porous carbons at the edge of a PAN-b-PMMA-CF.[146] Reprinted from Zhou *et al.*,[146] Copyright (2019), with permission from American Association for the Advancement of Science.

polymer in the system, as shown in Figure 12. As for the thermal/UV degradation of certain blocks, in 1996, Morkved *et al.* showed that the exposure of a film consisting of PS-*b*-PMMA to UV radiation led to the degradation of PMMA and the crosslinking of the PS phase.[145] Figure 12b displays UV radiation degradation of polymer B in an AB diblock copolymer to result in a structure created only by polymer A.[139] The success of UV degradation as a selective removal method to develop structured architectures in 2D and 3D systems could be used to generate internal structures of block copolymer-based 1D nanofiber systems.

Thermal degradation relies on heating a material well above its decomposition temperature, thus allowing the removal of volatile by-products while leaving desired voids. These voids are evidence of a nanoporous structure that could be used to develop internal structures within NFs.[139] In 2019, Zhou *et al.* used poly(acrylonitrile)-*b*-PMMA (PAN-*b*-PMMA) to create block copolymer-based porous carbon fibers through oxidation and self-assembly. Subsequently fibers were exposed to a pyrolysis process to selectively remove the sacrificial PMMA resulting in development of nanopores within the fiber (Figure 13).[146]

Ozonolysis utilizes the reactivity between ozone and alkene double bonds as a cleaving mechanism that allows for an easier removal of a sacrificial component.[147] Lee *et al.* reported the removal of polyisoprene (PI) within a poly (4-vinylphenyl-dimethyl-2-propoxysilane)-*b*-polyisoprene-*b*-poly(4-vinylphenyl-dimethyl-2-propoxysilane) (PPS-PI-PPS) block copolymer.[148] This approach has yet to be used to prepare NFs, and the technique seems attractive to develop nanostructures with wide potential applications.[139]

In selective removal through hydrolysis, compounds within a system are broken down due to a reaction with aqueous solvent to yield new products. In 1997, Liu *et al.* completed a partial removal of a sacrificial block within a block copolymer by hydrolysis. The significance of their work showed that porous materials can be created through the selective removal of a material through hydrolysis.[139,149] The selective removal of PLA within a poly(styrene-*stat*-butadiene)-*b*-PLA (P(S-s-B)-*b*-PLA) membrane was done through hydrolysis to result in porous nanostructures in work conducted by Hampu *et al.* in 2019.[150] Although conventional wisdom suggests minority block domains are most attractive for removal leaving behind the porous matrix block material, recent research has shown that matrix removal can also unexpectedly produce intact porous minority block materials.[151] These selective removal processes, though conducted on polymer membranes, could also possibly be used to develop complex porous morphologies within NFs.[150]

4.3. Fibers made from polymer blend-based systems

Polymer blends are mixtures, analogous to metal alloys, in which two polymers are combined to create a new material with enhanced physical/chemical properties.[152] The mixing of polymers is commonly used to meet property requirements related to toughness, thermal resistance, modulus, impact resistance, and stress resistance. Polymer blends can be divided into three categories: immiscible/heterogeneous, compatibilized, and miscible/homogenous blends. In immiscible blends, the polymers comprising the blend exist as separated, nearly pure phases, each of which exhibits thermophysical properties (e.g., glass transition and melting temperatures) near those of the pure components. Moreover, immiscible blends generally have mechanically weak interfaces between phases due to their thermodynamic incompatibility, and they do not comply with the thermodynamic conditions of phase stability discussed later. Compatibilized blends are immiscible blends with mechanical properties in between those of the individual polymers or in a manner that captures a desirable property of each component which makes up the blend. The added compatibilizers, such as block copolymers, bridge across and strengthen the interfaces between the phases,[153] and can additionally stabilize the phase structure of the blend. Miscible polymer blends are relatively rare and contain polymer components that possess slightly favorable enthalpic interactions, yielding a blend with a single-phase structure and intermediate properties.

A blend of immiscible polymers yields a phase-separated mixture, leading to low interfacial adhesion, which in turn yields poor mechanical properties. However, if the structure is stabilized with a compatibilizer, it can impart excellent properties to the final material. To achieve this, the interface can be modified in a process termed

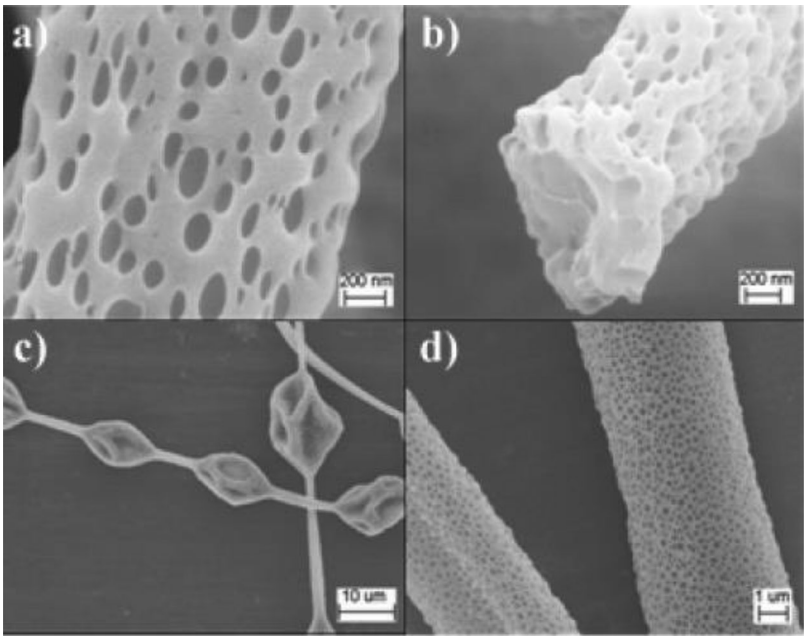

Figure 14. Porous fibers from aPMMA/MC from Mw of 350,000 g/mol (a) 10 wt % and (b) 12 wt % and from Mw of 996,000 g/mol (c) 10 wt % and (d) 12 wt%[156] Reprinted from Dayal *et al.*,[156] Copyright (2007), with permission from American Chemical Society.

compatibilization. There are two general methods for compatibilization: (1) incorporation of block/graft copolymers as polymeric "surfactants," and (2) reactive compatibilization, in which block or graft polymers are produced *in situ* by cross-reaction.[153] The former method is a non-reactive process in which copolymers anchor portions of their segments in each polymer. This reduces the interfacial tension and stabilizes the dispersion against coalescence. However, micellization within one or both phases can impede localization of the copolymer to the interface. The latter process is commercially more common, as it does not require additional components, and the copolymer is formed at the interface directly.

Dissolution, thermal decomposition, and phase separation processes are commonly used to remove polymer phases.[154] Phase separation of polymer components can occur during rapid solvent evaporation, which is a process characteristic of solution electrospinning processes. The reduction of solvent within a ternary polymer blend solution could result in the formation of two phases of different compositions. Phase separation could be achieved through vapor, nonsolvent, and thermally induced phase separation processes, known as VIPS, NIPS and TIPS, respectively.[155] It has recently been shown that the water vapor present in air could possibly lead to phase separation in some systems.[155] This could potentially create nanopores along the surface of NFs, which would lead to an increase in the surface-area-to-volume ratio (Figure 14).[156] TIPS has also been used to create nanopores upon cooling.[155] NIPS, also called immersion precipitation, has been used to generate nanopores by solvent/nonsolvent exchange.[155] This method of phase separation causes the polymer to precipitate after it is immersed in the

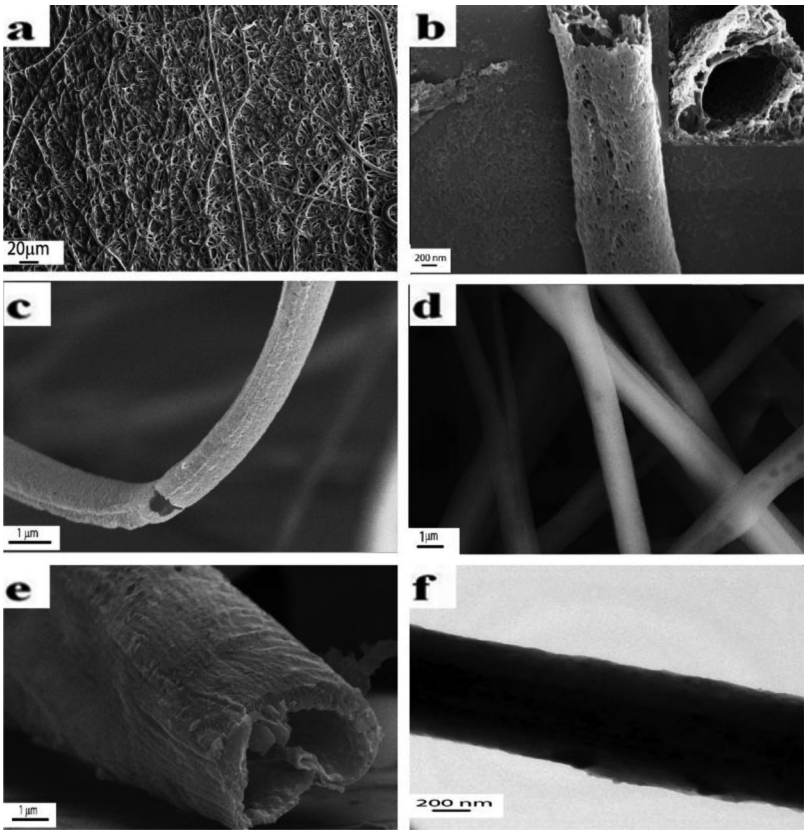

Figure 15. (a) FESEM image of porous hollow fibers collected in ethanol/acetone; (b) high magnification FESEM image of a single porous and hollow PAN fibers collected in ethanol/acetone mixture as shown in panel a. Inset shows cross-section of one of these fibers; (c) FESEM image of a single PAN fiber clearly showing the hollow nature of these fibers; (d) FESEM image of the PAN fibers collected on Si wafer and then dissolved in ethanol/acetone mixture; (e) image of a hollow PAN fiber collected with MEK as a collecting bath; (f) TEM image of core shell PAN/PMMA fibers[155] Reprinted from Nayani *et al.*,[155] Copyright (2012), with permission from American Chemical Society.

non-solvent bath, which results in unique nanostructures including porous and hollow porous fibers (Figure 15).[155]

Bognitzki *et al.* applied both dissolution and thermal degradation to polymer blends to showcase how each method can be used to create different nanoscale morphologies.[154] NFs were electrospun from combinations of polyvinylpyrrolidone (PVP) and either PLLA or PDLLA. Following electrospinning, highly porous structured fibers were developed using the dissolution of PVP with water.[154] The subsequent removal of one phase was promoted by high temperature annealing, resulting in the thermal decomposition of PLLA and PDLLA.[154] The fibers were annealed at 200 °C, well above the T_g and melting temperature of PLLA, resulting in the partial removal of the PLLA and causing the formation of droplets of PVP, yielding fluctuations in fiber diameter.[154]

Phase separation to manipulate the structure of NFs created by electrospinning various blends of polybutadiene (PB) and polycarbonate (PC), as well as PMMA and PS was reported by Wei *et al.*[157] As the ratio between the PB and PC was increased, there

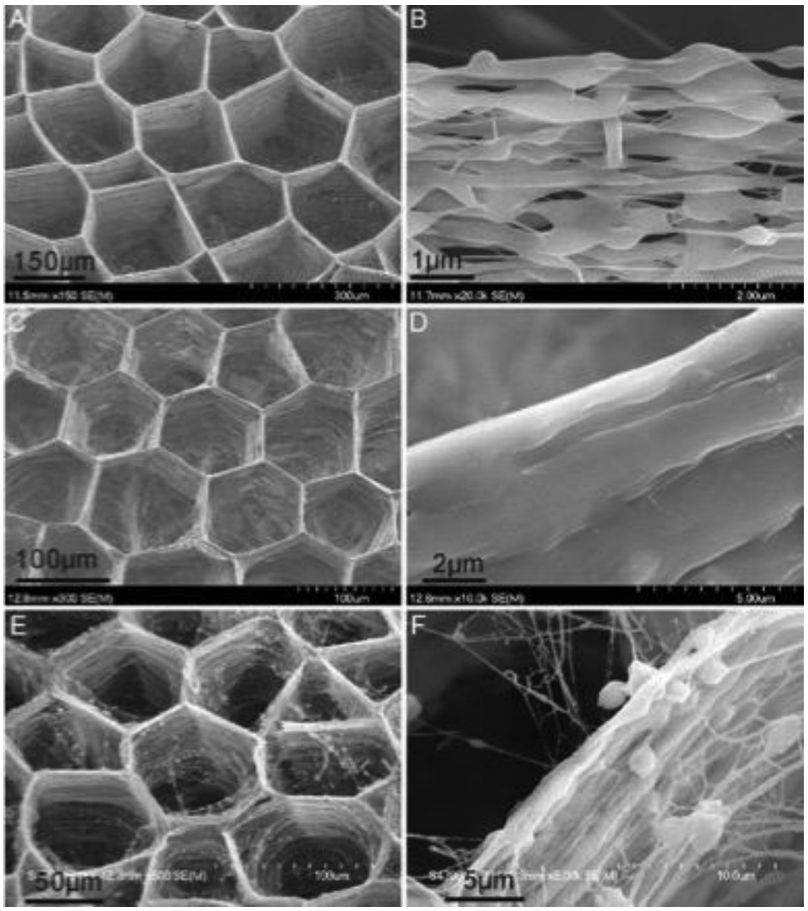

Figure 16. SEM images showing the surface morphology and wall structure of the HNFSs of PVA and PEO electrospun fibers at different conditions: (A,B) PVA, concentration 6%, 22 kV, on plastic films; (C,D) PEO, concentration 16%, 22 kV, on Al substrates; (E,F) PEO, concentration 16%, 19 kV, on aluminum substrates.[10] Reprinted from Yan *et al.*,[10] Copyright (2011), with permission from American Chemical Society.

was increased distinction of the core-shell structure within the fibers. Thus, the formation of the core-shell fibers was potentially caused by the different viscosities or solubilities of the polymers within the blend. Wei *et al.* found that larger solubility difference between the polymers in a blend yielded core-sheath structures, while smaller polymer solubility differences caused co-continuous structures.

Parreño *et al.* reported the use of polymer blends to manipulate external and internal fiber structures.[158] They studied blends of sulfur copolymers (sulfur 1,3 diisopropenyl benzene, (SDIB)) and polybenzoaxines (PBz) subjected to electrospinning.[158] As the SDIB concentration increased, the range of fiber diameters increased as well, and the fibers displayed less uniformity up to a saturation level where, given the high concentration of SDIB, a beads-on-string morphology resulted.[158] Mishra *et al.* were able to create NFs using blends of relatively hydrophobic poly(vinyl acetate) (PVAc) and hydrophilic poly(acrylic acid) (PAA).[114] Micro-compounding was used to blend the polymers in various compositions and then fibers were drawn directly from the melted

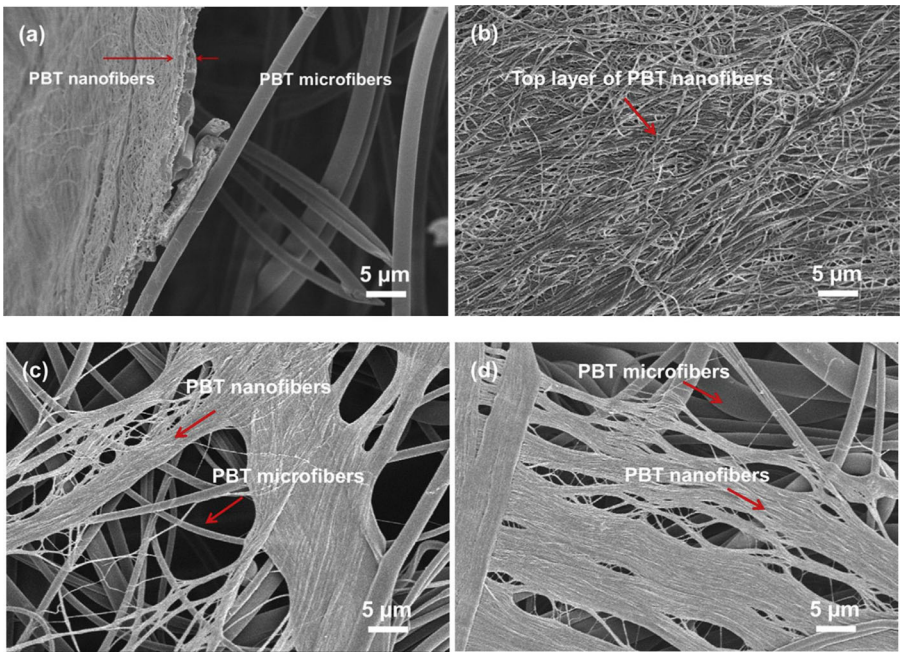

Figure 17. SEM images of (a) the side view of a double-layer nano-/micro-fiber composite where the top nanofiber layer was obtained by water-extraction of the melt-blown SP/PBT fibers collected for three collection rotations, (b) the top view of the nanofiber layer, (c) and (d) the top views of the double-layer composite demonstrating the overall porous structure after the collection was decreased from 3 rotations to 1 rotation[159] Reprinted from Wang *et al.*,[159] Copyright (2016), with permission from Elsevier.

blends.[114] They found that, contrary to the pure PVAc or PAA fragile fibers which had solid cross-sections and were difficult to melt spin, the blended PAA/PVAc fibers produced a system that could be melt-spun and resulted in porous fibers with honeycomb-like structures.[114] Though there is also a report available where Yan *et al.* have demonstrated how three different polymers can self-assemble into honeycomb patterned nanofibers structures using wet electrospinning method (Figure 16).[10] Wang *et al.* used an immiscible polymer blend to make melt-blown NFs inside microfibers, which were collected on a pre-melt-blown mat of microfibers.[159] They used a blend of majority sulfopolyester (SP) and minority poly(butylene terephthalate) (PBT), where the water-soluble SP was the "sacrificial phase." By melt blowing the immiscible blend, the PBT dispersed minority phase was drawn into NFs that were contained inside the SP microfiber matrix; after removal of the SP matrix following a water wash, an almost pure PBT nanofiber layer remained (Figure 17).[159] They created NFs with average diameters as small as 70 nm using an immiscible polymer blend, while avoiding the use of organic solvents.

Xu *et al.* used polymeric blends to create a 3-dimensional (3D) nanofibrous scaffold with pore sizes ranging from sub-microns to hundreds of microns.[160] As feedstock, PCL was blended with cellulose acetate (CA) using thermally induced self-agglomeration (TISA).[160] They submerged a glass bottle with short PCL NFs into a water bath close to the PCL melting point to promote nanofiber agglomeration and therefore form a 3D structure with interconnected/hierarchal pores; the system was afterwards freeze-dried

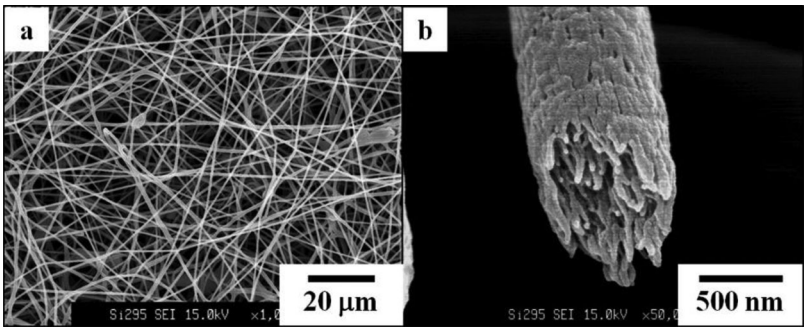

Figure 18. SEM images of the porous PAN NFs. The polymer blend ratio is PAN 10/PEG 8. (a) Overall and (b) magnified view of a fractured cross-section.[161] Reprinted from Nagamine *et al.*,[161] Copyright (2014), with permission from Elsevier.

yielding a 3D nanofibrous scaffold.[160] In this case the process altered the structure of the membrane itself by an interconnection of the developed fibers to form an aerogel type structure. Nagamine *et al.* created NFs with nanopores 10--20 nm in diameter using a blend of PAN and PEO (Figure 18).[161] Following electrospinning, the PEO was leached by water leaving porous PAN NFs that were used as templates for porous silica NFs.[161] A more complex structure can be created using surfactant molecules to create a micellar template; the team used the cationic surfactant, cetyltrimethylammonium chloride (CTAC), as an additional template to form an ordered mesopore (2–3 nm) structure.[161] Porous NFs such as these could have a myriad of applications including filtration, tissue engineering, and energy generation and storage.[161]

Porous carbon NFs (CNFs) were developed by Jo *et al.*[162] The team electrospun PAN blended with either PAA, PEO, PMMA, or PS; the resulting NFs were subsequently subjected to carbonization (Figure 19).[162] The CNF pore size was a function of the domain size of the dispersed phase (here, the pyrolyzing polymer) which was affected by the difference in the solubility parameters.[162] As the difference increased, the resulting pores were similarly larger.[162] For example, the PAN/PS combination had the greatest difference in solubility parameters and yielded the greatest pore size.[162]

Philip *et al.* electrospun a miscible polymer blend of PEO and PMMA using a chloroform-acetone mixture as solvent.[163] The developed fiber membrane was subjected to dissolution in deionized water for a few weeks. The resulting NFs exhibited roughness at the surface caused by the removal of PEO.[163] Kijeńska *et al.* developed electrospun core-shell NFs using a blend of poly(lactide-*co*-caprolactone) (PLCL) and laminin (ECM protein) dissolved in hexafluoro-2-propanol (HFP).[164] The shell comprised PLCL dissolved in HFP while the core consisted of the laminin dissolved in water.[164] NFs like these could be used to prevent the denaturization of proteins encapsulated by shell, or by having one protein in the core and one in the shell to yield controlled release.[164] Expanding on the previous application, Sedghi *et al.* were able to create core-shell NF mats using a coaxial electrospinning method; in one syringe, a blend of chitosan (CS) and PVA was used while the other compartment was filled with curcumin dissolved in ethanol.[165] The team found that as the amount of PVA in the PVA-CS blend was increased, the fiber uniformity increased (less beads were observed, together with a smoother fiber surface) (Figure 20).[165]

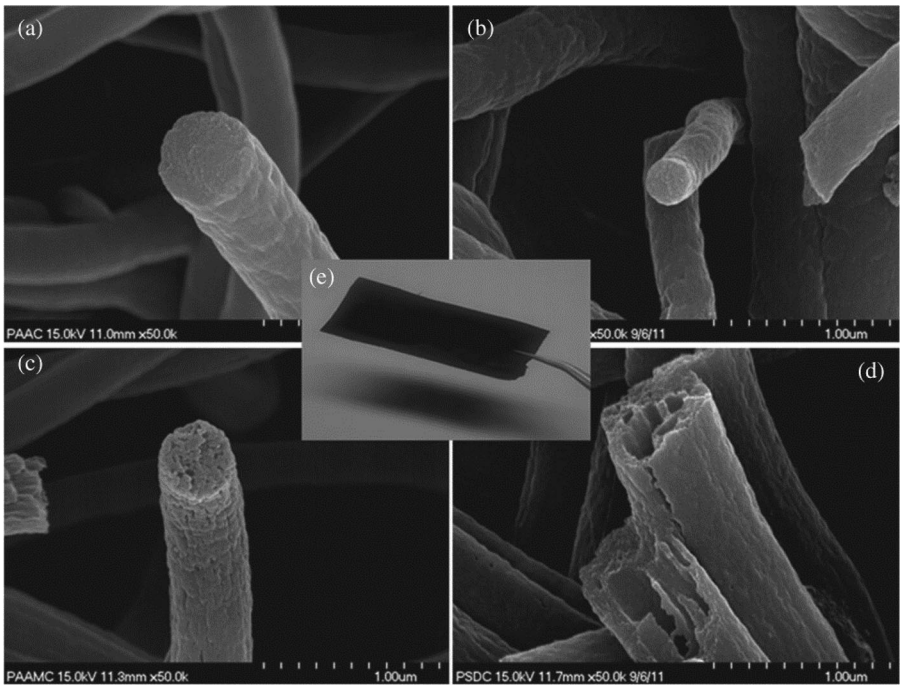

Figure 19. Cross-sectional SEM images of CNFs: (a) PAN/PAA; (b) PAN/PEG; (c) PAN/PMMA; (d) PAN/PS. (e) Optical image of sheet-type PAN/PMMA carbon web[162] Reprinted from Jo *et al.*,[162] Copyright (2014), with permission from Wiley.

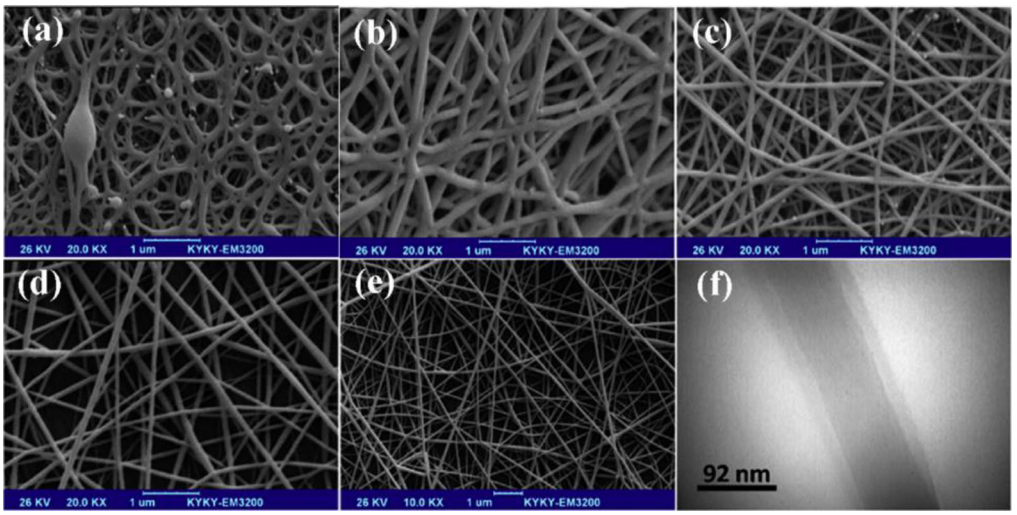

Figure 20. SEM images of F1 (a), F2 (b), F3(c), F4 blend NFs (d), F5 core/shell Cur/PVA-CS NFs (e) and TEM image of F5 NFs (f). The notation "Fn" refers to the different types of samples, such that F1, F2, F3, and F4 are a blended structure with increasing concentrations of PVA (wt%) of 5 wt%, 6 wt%, 7 wt%, and 8 wt%, respectively. F5 is a core-sheath structure with 8 wt% PVA.[165] Reprinted from Sedghi *et al.*,[165] Copyright (2016), with permission from Elsevier.

5. Conclusion and future scope

The ability to design NFs with different internal structures and surface morphologies provides an opportunity to develop special functions for advanced applications. A review on the effect of materials, processing techniques, and system selection, such as emulsion, block-copolymer, or blends, on fiber diameter, alignment, porosity, and overall internal nanofiber structure has been presented. The development of hollow, core-sheath, porous, gyroid, beaded and several other fiber structures has been described. These structures hold great promise in energy generation/storage, optoelectronics, water treatment, healthcare, food packaging, and biomedical applications. Most of the reported work has used electrospinning, which, until recently, dominated nanofiber production with large scale potential. This review presented detail on the tuning of internal structure of electrospun fibers designed from emulsions, block copolymers, and polymer blends as well as the effect of added surfactant, polymer, and/or solvent selection and processing parameters. As new nanofiber processing methods emerge such as Forcespinning®, which now operates at an industrial level, more studies will appear focusing on the analysis of materials and particular processing parameters such as rotational speed, nozzle diameter, and nozzle-collector distance, on the fiber internal structure and morphology.

In general hierarchical nanofiber design has abundant opportunities to be explored and significant growth may be expected. While the majority of the studies have used solvents for fiber processing, solvent-free methods are attractive but not yet frequently used/demonstrated. It will also be of interest how the effective methods to design internal structure such as those demonstrated in microfibers through, for example, melt-blowing, may be translated into prescribing the internal structure of NFs.

Acknowledgements

The authors acknowledge support received from National Science Foundation under PREM Award Number DMR-2122178 and MRSEC Award Number DMR-2011401.

Declaration of interest statement

The authors report there are no competing interests to declare.

Funding

This work was supported by NSF.

ORCID

Victoria Padilla http://orcid.org/0000-0002-4676-1337
Karen Lozano http://orcid.org/0000-0002-6676-8632

References

1. Agarwal, S.; Greiner, A.; Wendorff, J. H. Functional Materials by Electrospinning of Polymers. *Prog. Polym. Sci.* **2013**, *38*, 963–991. DOI: 10.1016/j.progpolymsci.2013.02.001.

2. Barnes, C. P.; Sell, S. A.; Boland, E. D.; Simpson, D. G.; Bowlin, G. L. Nanofiber Technology: Designing the Next Generation of Tissue Engineering Scaffolds. *Adv. Drug Delivery Rev.* **2007**, *59*, 1413–1433. DOI: 10.1016/j.addr.2007.04.022.
3. Zhang, L.; Aboagye, A.; Kelkar, A.; Lai, C.; Fong, H. A Review: Carbon Nanofibers from Electrospun Polyacrylonitrile and Their Applications. *J. Mater. Sci.* **2014**, *49*, 463–480. DOI: 10.1007/s10853-013-7705-y.
4. Hu, X.; Liu, S.; Zhou, G.; Huang, Y.; Xie, Z.; Jing, X. Electrospinning of Polymeric Nanofibers for Drug Delivery Applications. *J. Control. Release* **2014**, *185*, 12–21. DOI: 10.1016/j.jconrel.2014.04.018.
5. Leung, V.; Ko, F. Biomedical Applications of Nanofibers. *Polym. Adv. Technol.* **2011**, *22*, 350–365. DOI: 10.1002/pat.1813.
6. Xue, J.; Wu, T.; Dai, Y.; Xia, Y. Electrospinning and Electrospun Nanofibers: Methods, Materials, and Applications. *Chem. Rev.* **2019**, *119*, 5298–5415. DOI: 10.1021/acs.chemrev.8b00593.
7. Sarier, N.; Arat, R.; Menceloglu, Y.; Onder, E.; Boz, E. C.; Oguz, O. Production of PEG Grafted PAN Copolymers and Their Electrospun Nanowebs as Novel Thermal Energy Storage Materials. *Thermochim. Acta* **2016**, *643*, 83–93. DOI: 10.1016/j.tca.2016.10.002.
8. Li, K.; Clarkson, C. M.; Wang, L.; Liu, Y.; Lamm, M.; Pang, Z.; Zhou, Y.; Qian, J.; Tajvidi, M.; Gardner, D. J.; et al. Alignment of Cellulose Nanofibers: Harnessing Nanoscale Properties to Macroscale Benefits. *ACS Nano.* **2021**, *15*, 3646–3673. DOI: 10.1021/acsnano.0c07613.
9. Zhang, D.; Chang, J. Patterning of Electrospun Fibers Using Electroconductive Templates. *Adv. Mater.* **2007**, *19*, 3664–3667. DOI: 10.1002/adma.200700896.
10. Yan, G.; Yu, J.; Qiu, Y.; Yi, X.; Lu, J.; Zhou, X.; Bai, X. Self-Assembly of Electrospun Polymer Nanofibers: A General Phenomenon Generating Honeycomb-Patterned Nanofibrous Structures. *Langmuir* **2011**, *27*, 4285–4289. DOI: 10.1021/la1047936.
11. Braghirolli, D. I.; Steffens, D.; Pranke, P. Electrospinning for Regenerative Medicine: A Review of the Main Topics. *Drug Discov. Today.* **2014**, *19*, 743–753. DOI: 10.1016/j.drudis.2014.03.024.
12. Huang, Z.-M.; Zhang, Y. Z.; Kotaki, M.; Ramakrishna, S. A Review on Polymer Nanofibers by Electrospinning and Their Applications in Nanocomposites. *Compos. Sci. Technol.* **2003**, *63*, 2223–2253. DOI: 10.1016/S0266-3538(03)00178-7.
13. Lasprilla-Botero, J.; Alvarez-Lainez, M.; Lagaron, J. M. The Influence of Electrospinning Parameters and Solvent Selection on the Morphology and Diameter of Polyimide Nanofibers. *Mater. Today Commun.* **2018**, *14*, 1–9. DOI: 10.1016/j.mtcomm.2017.12.003.
14. Nataraj, S. K.; Yang, K. S.; Aminabhavi, T. M. Polyacrylonitrile-Based Nanofibers-A State-of-the-Art Review. *Prog. Polym. Sci.* **2012**, *37*, 487–513. DOI: 10.1016/j.progpolymsci.2011.07.001.
15. Soltani, S.; Khanian, N.; Choong, T. S. Y.; Rashid, U. Recent Progress in the Design and Synthesis of Nanofibers with Diverse Synthetic Methodologies: Characterization and Potential Applications. *New J. Chem.* **2020**, *44*, 9581–9606. DOI: 10.1039/D0NJ01071E.
16. Ma, P. X. Scaffolds for Tissue Fabrication. *Mater. Today* **2004**, *7*, 30–40. DOI: 10.1016/S1369-7021(04)00233-0.
17. Li, D.; Xia, Y. Electrospinning of Nanofibers: Reinventing the Wheel? *Adv. Mater.* **2004**, *16*, 1151–1170. DOI: 10.1002/adma.200400719.
18. Zhang, C.; Xue, X.; Luo, Q.; Li, Y.; Yang, K.; Zhuang, X.; Jiang, Y.; Zhang, J.; Liu, J.; Zou, G.; Liang, X.-J. Self-Assembled Peptide Nanofibers Designed as Biological Enzymes for Catalyzing Ester Hydrolysis. *ACS Nano.* **2014**, *8*, 11715–11723. DOI: 10.1021/nn5051344.
19. Martin, C. R. Template Synthesis of Electronically Conductive Polymer Nanostructures. *Acc. Chem. Res.* **1995**, *28*, 61–68. DOI: 10.1021/ar00050a002.
20. Sarkar, K.; Gomez, C.; Zambrano, S.; Ramirez, M.; de Hoyos, E.; Vasquez, H.; Lozano, K. Electrospinning to Forcespinning. *Mater. Today* **2010**, *13*, 12–14. DOI: 10.1016/S1369-7021(10)70199-1.

21. Ondarcuhu, T.; Joachim, C. Drawing a Single Nanofibre over Hundreds of Microns. *Europhys. Lett.* **1998**, *42*, 215–220. DOI: 10.1209/epl/i1998-00233-9.
22. Feng, L.; Li, S.; Li, H.; Zhai, J.; Song, Y.; Jiang, L.; Zhu, D. Super-Hydrophobic Surface of Aligned Polyacrylonitrile Nanofibers. *Angew. Chem. Int. Ed.* **2002**, *41*, 1221–1223. DOI: 10.1002/1521-3773(20020402)41:7<1221::AID-ANIE1221>3.0.CO;2-G.
23. Wang, J.; Zhang, D. One-Dimensional Nanostructured Polyaniline: Syntheses, Morphology Controlling, Formation Mechanisms, New Features, and Applications. *Adv. Polym. Technol.* **2013**, *32*, E323–E368. DOI: 10.1002/adv.21283.
24. Ma, P. X.; Zhang, R. Synthetic Nanoscale Fibrous Extracellular Matrix. *J. Biomed. Mater. Res.* **1999**, *46*, 60–72. DOI: 10.1002/(SICI)1097-4636(199907)46:1<60::AID-JBM7>3.0.CO;2-H.
25. Whitesides, G. M.; Grzybowski, B. Self-Assembly at All Scales. *Science* **2002**, *295*, 2418–2421. DOI: 10.1126/science.1070821.
26. Hartgerink, J. D.; Beniash, E.; Stupp, S. I. Self-Assembly and Mineralization of Peptide-Amphiphile Nanofibers. *Science* **2001**, *294*, 1684–1688. DOI: 10.1126/science.1063187.
27. Zhang, S. Fabrication of Novel Biomaterials through Molecular Self-Assembly. *Nat. Biotechnol.* **2003**, *21*, 1171–1178. DOI: 10.1038/nbt874.
28. Yao, J.; Bastiaansen, C. W. M.; Peijs, T. High Strength and High Modulus Electrospun Nanofibers. *Fibers* **2014**, *2*, 158–186. DOI: 10.3390/fib2020158.
29. Greiner, A.; Wendorff, J. H. Electrospinning: A Fascinating Method for the Preparation of Ultrathin Fibers. *Angew. Chem. Int. Ed. Engl.* **2007**, *46*, 5670–5703. DOI: 10.1002/anie.200604646.
30. Li, W.-J.; Laurencin, C. T.; Caterson, E. J.; Tuan, R. S.; Ko, F. K. Electrospun Nanofibrous Structure: A Novel Scaffold for Tissue Engineering. *J. Biomed. Mater. Res.* **2002**, *60*, 613–621.
31. Araujo, T. M.; Sinha-Ray, S.; Pegoretti, A.; Yarin, A. L. Electrospinning of a Blend of a Liquid Crystalline Polymer with Poly(Ethylene Oxide): Vectran Nanofiber Mats and Their Mechanical Properties. *J. Mater. Chem. C* **2013**, *1*, 351–358. DOI: 10.1039/C2TC00048B.
32. Yao, J.; Jin, J.; Lepore, E.; Pugno, N. M.; Bastiaansen, C. W. M.; Peijs, T. Electrospinning of p-Aramid Fibers. *Macromol. Mater. Eng.* **2015**, *300*, 1238–1245. DOI: 10.1002/mame.201500130.
33. Bognitzki, M.; Czado, W.; Frese, T.; Schaper, A.; Hellwig, M.; Steinhart, M.; Greiner, A.; Wendorff, J. H. Nanostructured Fibers via Electrospinning. *Adv. Mater.* **2001**, *13*, 70–72. DOI: 10.1002/1521-4095(200101)13:1<70::AID-ADMA70>3.0.CO;2-H.
34. Li, D.; Xia, Y. Fabrication of Titania Nanofibers by Electrospinning. *Nano Lett.* **2003**, *3*, 555–560. DOI: 10.1021/nl034039o.
35. Yoshimoto, H.; Shin, Y. M.; Terai, H.; Vacanti, J. P. A Biodegradable Nanofiber Scaffold by Electrospinning and Its Potential for Bone Tissue Engineering. *Biomaterials* **2003**, *24*, 2077–2082. DOI: 10.1016/S0142-9612(02)00635-X.
36. Shambaugh, R. L. A Macroscopic View of the Melt-Blowing Process for Producing Microfibers. *Ind. Eng. Chem. Res.* **1988**, *27*, 2363–2372. DOI: 10.1021/ie00084a021.
37. Ellison, C. J.; Phatak, A.; Giles, D. W.; Macosko, C. W.; Bates, F. S. Melt Blown Nanofibers: Fiber Diameter Distributions and Onset of Fiber Breakup. *Polymer* **2007**, *48*, 3306–3316. DOI: 10.1016/j.polymer.2007.04.005.
38. Bresee, R. R.; Ko, W.-C. Fiber Formation during Melt Blowing. *Int. Nonwovens J.* **2003**, *12*, 21–28.
39. Fridrikh, S. V.; Yu, J. H.; Brenner, M. P.; Rutledge, G. C. Controlling the Fiber Diameter during Electrospinning. *Phys. Rev. Lett.* **2003**, *90*, 144502.
40. Fridrikh, S. V.; Yu, J. H.; Brenner, M. P.; Rutledge, G. C. Nonlinear Whipping Behavior of Electrified Fluid Jets. *ACS Symp. Ser.* **2006**, *918*, 36–55.
41. Nayak, R.; Padhye, R.; Kyratzis, I. L.; Truong, Y. B.; Arnold, L. Recent Advances in Nanofiber Fabrication Techniques. *Text. Res. J.* **2012**, *82*, 129–147. DOI: 10.1177/0040517511424524.

42. Hassan, M. A.; Yeom, B. Y.; Wilkie, A.; Pourdeyhimi, B.; Khan, S. A. Fabrication of Nanofiber Meltblown Membranes and Their Filtration Properties. *J. Membr. Sci.* **2013**, *427*, 336–344. DOI: 10.1016/j.memsci.2012.09.050.
43. Jin, K.; Eyer, S.; Dean, W.; Kitto, D.; Bates, F. S.; Ellison, C. J. Bimodal Nanofiber and Microfiber Nonwovens by Melt-Blowing Immiscible Ternary Polymer Blends. *Ind. Eng. Chem. Res.* **2020**, *59*, 5238–5246. DOI: 10.1021/acs.iecr.9b04887.
44. Zuo, F.; Tan, D. H.; Wang, Z.; Jeung, S.; Macosko, C. W.; Bates, F. S. Nanofibers from Melt Blown Fiber-in-Fiber Polymer Blends. *ACS Macro Lett.* **2013**, *2*, 301–305.
45. Banerji, A.; Jin, K.; Mahanthappa, M. K.; Bates, F. S.; Ellison, C. J. Porous Fibers Templated by Melt Blowing Cocontinuous Immiscible Polymer Blends. *ACS Macro Lett.* **2021**, *10*, 1196–1203. DOI: 10.1021/acsmacrolett.1c00456.
46. Xue, J.; Xie, J.; Liu, W.; Xia, Y. Electrospun Nanofibers: New Concepts, Materials, and Applications. *Acc. Chem. Res.* **2017**, *50*, 1976–1987. DOI: 10.1021/acs.accounts.7b00218.
47. Sun, B.; Long, Y. Z.; Zhang, H. D.; Li, M. M.; Duvail, J. L.; Jiang, X. Y.; Yin, H. L. Advances in Three-Dimensional Nanofibrous Macrostructures via Electrospinning. *Prog. Polym. Sci.* **2014**, *39*, 862–890. DOI: 10.1016/j.progpolymsci.2013.06.002.
48. Liao, Y.; Loh, C.-H.; Tian, M.; Wang, R.; Fane, A. G. Progress in Electrospun Polymeric Nanofibrous Membranes for Water Treatment: Fabrication, Modification and Applications. *Prog. Polym. Sci.* **2018**, *77*, 69–94. DOI: 10.1016/j.progpolymsci.2017.10.003.
49. Luo, C. J.; Stoyanov, S. D.; Stride, E.; Pelan, E.; Edirisinghe, M. Electrospinning versus r Methods: From Specifics to Technological Convergence. *Chem. Soc. Rev.* **2012**, *41*, 4708–4735. DOI: 10.1039/c2cs35083a.
50. Jirsak, O.; Sanetrnik, F.; Lukas, D.; Kotek, V.; Martinova, L.; Chaloupek, J. Process and Apparatus for Producing Nanofibers from Polymer Solution by Electrostatic Spinning. Technicka Univerzita v Liberci, Czech Rep. **2004**, 13 pp.
51. Padilla-Gainza, V.; Morales, G.; Rodriguez-Tobias, H.; Lozano, K. Forcespinning Technique for the Production of Poly(D,L-Lactic Acid) Submicrometer Fibers: Process-Morphology-Properties Relationship. *J. Appl. Polym. Sci.* **2019**, *136*, 47643. DOI: 10.1002/app.47643.
52. Barbosa, R.; Gupta, S. K.; Srivastava, B. B.; Villarreal, A.; De Leon, H.; Peredo, M.; Bose, S.; Lozano, K. Bright and Persistent Green and Red Light-Emitting Fine Fibers: A Potential Candidate for Smart Textiles. *J. Lumin.* **2021**, *231*, 117760. DOI: 10.1016/j.jlumin.2020.117760.
53. Simonet, M.; Schneider, O. D.; Neuenschwander, P.; Stark, W. J. Ultraporous 3D Polymer Meshes by Low-Temperature Electrospinning: Use of Ice Crystals as a Removable Void Template. *Polym. Eng. Sci.* **2007**, *47*, 2020–2026. DOI: 10.1002/pen.20914.
54. Vaquette, C.; Cooper-White, J. J. Increasing Electrospun Scaffold Pore Size with Tailored Collectors for Improved Cell Penetration. *Acta Biomater.* **2011**, *7*, 2544–2557. DOI: 10.1016/j.actbio.2011.02.036.
55. Rampichova, M.; Chvojka, J.; Buzgo, M.; Prosecka, E.; Mikes, P.; Vyslouzilova, L.; Tvrdik, D.; Kochova, P.; Gregor, T.; Lukas, D.; Amler, E. Elastic Three-Dimensional Poly (ε-Caprolactone) Nanofibre Scaffold Enhances Migration, Proliferation and Osteogenic Differentiation of Mesenchymal Stem Cells. *Cell Prolif.* **2013**, *46*, 23–37. DOI: 10.1111/cpr.12001.
56. Blakeney, B. A.; Tambralli, A.; Anderson, J. M.; Andukuri, A.; Lim, D.-J.; Dean, D. R.; Jun, H.-W. Cell Infiltration and Growth in a Low Density, Uncompressed Three-Dimensional Electrospun Nanofibrous Scaffold. *Biomaterials* **2011**, *32*, 1583–1590. DOI: 10.1016/j.biomaterials.2010.10.056.
57. Sill, T. J.; von Recum, H. A. Electrospinning: Applications in Drug Delivery and Tissue Engineering. *Biomaterials* **2008**, *29*, 1989–2006. DOI: 10.1016/j.biomaterials.2008.01.011.
58. Omer, S.; Forgách, L.; Zelkó, R.; Sebe, I. Scale-up of Electrospinning: Market Overview of Products and Devices for Pharmaceutical and Biomedical Purposes. *Pharmaceutics* **2021**, *13*, 286. DOI: 10.3390/pharmaceutics13020286.

59. Buzgo, M.; Rampichova, M.; Vocetkova, K.; Sovkova, V.; Lukasova, V.; Doupnik, M.; Mickova, A.; Rustichelli, F.; Amler, E. Emulsion Centrifugal Spinning for Production of 3D Drug Releasing Nanofibres with Core/Shell Structure. *RSC Adv.* **2017**, *7*, 1215–1228. DOI: 10.1039/C6RA26606A.
60. Lozano, K.; Sarkar, K. Superfine Fiber Creating Spinneret for Spinning Superfine Fibers of Micron and Submicron Size Diameters and Nanofibers and Spinning Apparatus Therefor and Uses Thereof. The University of Texas System, USA, **2009**, 47 pp.
61. Zhang, X.; Lu, Y. Centrifugal Spinning: An Alternative Approach to Fabricate Nanofibers at High Speed and Low Cost. *Polym. Rev.* **2014**, *54*, 677–701. DOI: 10.1080/15583724.2014.935858.
62. Peno, E.; Lipton, R. Apparatuses and Methods for the Simultaneous Production of Microfibers and Nanofibers. Fibrerio Technology Corporation, USA, **2012**, 51 pp.
63. Peno, E.; Lipton, R. Devices and Methods for the Production of Coaxial Microfibers and Nanofibers. Fiberio Technology Corporation, USA, **2012**, 47 pp.
64. Peno, E.; Lipton, R.; Kay, S. Apparatuses and Methods for Production of Microfibers and Nanofibers. Fiberio Technology Corporation, USA, **2012**, 51 pp.
65. Caruntu, D. I.; Padron, S.; Lozano, K. Two-Dimensional Modeling of Nonlinear Dynamics of Forcespinning Jet Formation. *J. Comput. Nonlinear Dyn* **2021**, *16*, 081006.
66. Sebe, I.; Szabo, B.; Nagy, Z. K.; Szabo, D.; Zsidai, L.; Kocsis, B.; Zelko, R. Polymer Structure and Antimicrobial Activity of Polyvinylpyrrolidone-Based Iodine Nanofibers Prepared with High-Speed Rotary Spinning Technique. *Int. J. Pharm.* **2013**, *458*, 99–103. DOI: 10.1016/j.ijpharm.2013.10.011.
67. Padron, S.; Fuentes, A.; Caruntu, D.; Lozano, K. Experimental Study of Nanofiber Production through Forcespinning. *J. Appl. Phys.* **2013**, *113*, 024318. DOI: 10.1063/1.4769886.
68. Padron, S.; Patlan, R.; Gutierrez, J.; Santos, N.; Eubanks, T.; Lozano, K. Production and Characterization of Hybrid BEH-PPV/PEO Conjugated Polymer Nanofibers by Forcespinning. *J. Appl. Polym. Sci.* **2012**, *125*, 3610–3616. DOI: 10.1002/app.36420.
69. Raghavan, B.; Soto, H.; Lozano, K. Fabrication of Melt Spun Polypropylene Nanofibers by Forcespinning. *J. Eng. Fibers Fabr.* **2013**, *8*, 155892501300800. DOI: 10.1177/155892501300800106.
70. Yan, J.; Han, Y.; Xia, S.; Wang, X.; Zhang, Y.; Yu, J.; Ding, B. Polymer Template Synthesis of Flexible $BaTiO_3$ Crystal Nanofibers. *Adv. Funct. Mater.* **2019**, *29*, 1907919. DOI: 10.1002/adfm.201907919.
71. Tao, S. L.; Desai, T. A. Aligned Arrays of Biodegradable Poly(ε-Caprolactone) Nanowires and Nanofibers by Template Synthesis. *Nano Lett.* **2007**, *7*, 1463–1468. DOI: 10.1021/nl0700346.
72. Pender, M. J.; Sneddon, L. G. An Efficient Template Synthesis of Aligned Boron Carbide Nanofibers Using a Single-Source Molecular Precursor. *Chem. Mater.* **2000**, *12*, 280–283. DOI: 10.1021/cm990657n.
73. Vasita, R.; Katti, D. S. Nanofibers and Their Applications in Tissue Engineering. *Int. J. Nanomed.* **2006**, *1*, 15–30. DOI: 10.2147/nano.2006.1.1.15.
74. Liao, H.-S.; Lin, J.; Liu, Y.; Huang, P.; Jin, A.; Chen, X. Self-Assembly Mechanisms of Nanofibers from Peptide Amphiphiles in Solution and on Substrate Surfaces. *Nanoscale* **2016**, *8*, 14814–14820. DOI: 10.1039/c6nr04672j.
75. Li, W.-J.; Shanti, R.; Tuan, R. Electrospinning Technology for Nanofibrous Scaffolds in Tissue Engineering. In: *Nanotechnologies for the Life Sciences*; Kumar C.S.S.R. Ed.; Wiley Online Library, **2007**. DOI: 10.1002/9783527610419.ntls0097.
76. Zahmatkeshan, M.; Adel, M.; Bahrami, S.; Esmaeili, F.; Mahdi, S.; Yousef, R.; Bita, S.; Seyed, M.; Jameie, B.; Ashtari, K. Polymer Based Nanofibers: Preparation, Fabrication, and Applications. In: *Handbook of Nanofibers*; Barhoum, A., Bechelany, M., Makhlouf, A., Eds.; Springer: Cham, **2019**; *9*, pp 215–261.
77. Zhao, J.; Han, W.; Tu, M.; Huan, S.; Zeng, R.; Wu, H.; Cha, Z.; Zhou, C. Preparation and Properties of Biomimetic Porous Nanofibrous Poly(l-Lactide) Scaffold with Chitosan

Nanofiber Network by a Dual Thermally Induced Phase Separation Technique. *Mater. Sci. Eng. C Mater. Biol. Appl.* **2012**, *32*, 1496–1502. DOI: 10.1016/j.msec.2012.04.031.
78. Technology/Machinery FibeRio Technology Named in Global Cleantech 100. https://www.innovationintextiles.com/fiberio-technology-named-in-global-cleantech-100/. **2013**.
79. He, J.-H.; Wu, Y.; Zuo, W.-W. Critical Length of Straight Jet in Electrospinning. *Polymer* **2005**, *46*, 12637–12640. DOI: 10.1016/j.polymer.2005.10.130.
80. Li, D.; Wang, Y.; Xia, Y. Electrospinning of Polymeric and Ceramic Nanofibers as Uniaxially Aligned Arrays. *Nano Lett.* **2003**, *3*, 1167–1171. DOI: 10.1021/nl0344256.
81. Deitzel, J. M.; Kleinmeyer, J. D.; Hirvonen, J. K.; Beck Tan, N. C. Controlled Deposition of Electrospun Poly(Ethylene Oxide) Fibers. *Polymer* **2001**, *42*, 8163–8170. DOI: 10.1016/S0032-3861(01)00336-6.
82. Dersch, R.; Liu, T.; Schaper, A. K.; Greiner, A.; Wendorff, J. H. Electrospun Nanofibers: Internal Structure and Intrinsic Orientation. *J. Polym. Sci. A Polym. Chem.* **2003**, *41*, 545–553. DOI: 10.1002/pola.10609.
83. Sun, Z.; Zussman, E.; Yarin, A. L.; Wendorff, J. H.; Greiner, A. Compound Core–Shell Polymer Nanofibers by Co-Electrospinning. *Adv. Mater.* **2003**, *15*, 1929–1932. DOI: 10.1002/adma.200305136.
84. Xu, X.; Zhuang, X.; Chen, X.; Wang, X.; Yang, L.; Jing, X. Preparation of Core-Sheath Composite Nanofibers by Emulsion Electrospinning. *Macromol. Rapid Commun.* **2006**, *27*, 1637–1642. DOI: 10.1002/marc.200600384.
85. Tiwari, S. K.; Tzezana, R.; Zussman, E.; Venkatraman, S. S. Optimizing Partition-Controlled Drug Release from Electrospun Core–Shell Fibers. *Int. J. Pharm.* **2010**, *392*, 209–217. DOI: 10.1016/j.ijpharm.2010.03.021.
86. Jiang, H.; Wang, L.; Zhu, K. Coaxial Electrospinning for Encapsulation and Controlled Release of Fragile Water-Soluble Bioactive Agents. *J. Control. Release* **2014**, *193*, 296–303. DOI: 10.1016/j.jconrel.2014.04.025.
87. Zupančič, Š. Core-Shell Nanofibers as Drug Delivery Systems. *Acta Pharm.* **2019**, *69*, 131–153.
88. Sahoo, S.; Ang, L. T.; Goh, J. C.-H.; Toh, S.-L. Growth Factor Delivery through Electrospun Nanofibers in Scaffolds for Tissue Engineering Applications. *J. Biomed. Mater. Res. A* **2010**, *93*, 1539–1550. DOI: 10.1002/jbm.a.32645.
89. Jia, X.; Zhao, C.; Li, P.; Zhang, H.; Huang, Y.; Li, H.; Fan, J.; Feng, W.; Yuan, X.; Fan, Y. Sustained Release of VEGF by Coaxial Electrospun Dextran/PLGA Fibrous Membranes in Vascular Tissue Engineering. *J. Biomater. Sci. Polym. Ed.* **2011**, *22*, 1811–1827. DOI: 10.1163/092050610X528534.
90. Elahi, F.; Lu, W.; Guan, G.; Khan, F. Core-Shell Fibers for Biomedical Applications – A Review. *J. Bioeng. Biomed. Sci.* **2013**, *3*, 121/1–121/14.
91. Konno, M.; Kishi, Y.; Tanaka, M.; Kawakami, H. Core/Shell-Like Structured Ultrafine Branched Nanofibers Created by Electrospinning. *Polym. J.* **2014**, *46*, 792–799. DOI: 10.1038/pj.2014.74.
92. Arabpour, Z.; Baradaran- Rafii, A.; Bakhshaiesh, N. L.; Ai, J.; Ebrahimi-Barough, S.; Esmaeili Malekabadi, H.; Nazeri, N.; Vaez, A.; Salehi, M.; Sefat, F.; Ostad, S. N. Design and Characterization of Biodegradable Multi Layered Electrospun Nanofibers for Corneal Tissue Engineering Applications. *J. Biomed. Mater. Res. A* **2019**, *107*, 2340–2349. DOI: 10.1002/jbm.a.36742.
93. Han, D.; Steckl, A. J.; Serra, R.; Gorelick, N.; Fatima, U.; Brem, H.; Tyler, B.; Eberhart, C. G.; Brem, H. Multi-Layered Core-Sheath Fiber Membranes for Controlled Drug Release in the Local Treatment of Brain Tumor. *Sci. Rep.* **2019**, *9*, 17936.
94. Ruotsalainen, T.; Turku, J.; Heikkilä, P.; Ruokolainen, J.; Nykänen, A.; Laitinen, T.; Torkkeli, M.; Serimaa, R.; ten Brinke, G.; Harlin, A.; Ikkala, O. Towards Internal Structuring of Electrospun Fibers by Hierarchical Self-Assembly of Polymeric Comb-Shaped Supramolecules. *Adv. Mater.* **2005**, *17*, 1048–1052. DOI: 10.1002/adma.200401530.

95. Kalra, V.; Kakad, P. A.; Mendez, S.; Ivannikov, T.; Kamperman, M.; Joo, Y. L. Self-Assembled Structures in Electrospun Poly(Styrene-Block-Isoprene) Fibers. *Macromolecules* **2006**, *39*, 5453–5457. DOI: 10.1021/ma052643a.
96. Ma, M.; Krikorian, V.; Yu, J. H.; Thomas, E. L.; Rutledge, G. C. Electrospun Polymer Nanofibers with Internal Periodic Structure Obtained by Microphase Separation of Cylindrically Confined Block Copolymers. *Nano Lett.* **2006**, *6*, 2969–2972.
97. Li, D.; Tao, L.; Shen, Y.; Sun, B.; Xie, X.; Ke, Q.; Mo, X.; Deng, B. Fabrication of Multilayered Nanofiber Scaffolds with a Highly Aligned Nanofiber Yarn for Anisotropic Tissue Regeneration. *ACS Omega.* **2020**, *5*, 24340–24350. DOI: 10.1021/acsomega.0c02554.
98. Zhu, Y.; Leong, M. F.; Ong, W. F.; Chan-Park, M. B.; Chian, K. S. Esophageal Epithelium Regeneration on Fibronectin Grafted Poly(l-Lactide-Co-Caprolactone) (PLLC) Nanofiber Scaffold. *Biomaterials* **2007**, *28*, 861–868. DOI: 10.1016/j.biomaterials.2006.09.051.
99. Patel, A. C.; Li, S.; Wang, C.; Zhang, W.; Wei, Y. Electrospinning of Porous Silica Nanofibers Containing Silver Nanoparticles for Catalytic Applications. *Chem. Mater.* **2007**, *19*, 1231–1238. DOI: 10.1021/cm061331z.
100. Tan, S. T.; Wendorff, J. H.; Pietzonka, C.; Jia, Z. H.; Wang, G. Q. Biocompatible and Biodegradable Polymer Nanofibers Displaying Superparamagnetic Properties. *Chemphyschem* **2005**, *6*, 1461–1465. DOI: 10.1002/cphc.200500167.
101. Wang, X.; Ding, B.; Yu, J.; Wang, M.; Pan, F. A Highly Sensitive Humidity Sensor Based on a Nanofibrous Membrane Coated Quartz Crystal Microbalance. *Nanotechnology* **2010**, *21*, 055502. DOI: 10.1088/0957-4484/21/5/055502.
102. Kim, C.; Song, G.; Luo, L.; Cheong, J. Y.; Cho, S.-H.; Kwon, D.; Choi, S.; Jung, J.-W.; Wang, C.-M.; Kim, I.-D.; Park, S. Stress-Tolerant Nanoporous Germanium Nanofibers for Long Cycle Life Lithium Storage with High Structural Stability. *ACS Nano.* **2018**, *12*, 8169–8176. DOI: 10.1021/acsnano.8b03278.
103. Lin, J.; Ding, B.; Yu, J.; Hsieh, Y. Direct Fabrication of Highly Nanoporous Polystyrene Fibers via Electrospinning. *ACS Appl. Mater. Interfaces.* **2010**, *2*, 521–528. DOI: 10.1021/am900736h.
104. Zhang, Z.; Li, X.; Wang, C.; Fu, S.; Liu, Y.; Shao, C. Polyacrylonitrile and Carbon Nanofibers with Controllable Nanoporous Structures by Electrospinning. *Macromol. Mater. Eng.* **2009**, *294*, 673–678. DOI: 10.1002/mame.200900076.
105. Hou, H.; Wang, L.; Gao, F.; Wei, G.; Tang, B.; Yang, W.; Wu, T. General Strategy for Fabricating Thoroughly Mesoporous Nanofibers. *J. Am. Chem. Soc.* **2014**, *136*, 16716–16719. DOI: 10.1021/ja508840c.
106. Elishav, O.; Shener, Y.; Beilin, V.; Shter, G. E.; Ng, B.; Mustain, W. E.; Landau, M. V.; Herskowitz, M.; Grader, G. S. Electrospun Nanofibers with Surface Oriented Lamellar Patterns and Their Potential Applications. *Nanoscale* **2020**, *12*, 12993–13000. DOI: 10.1039/d0nr02641g.
107. Ma, M.; Titievsky, K.; Thomas, E. L.; Rutledge, G. C. Continuous Concentric Lamellar Block Copolymer Nanofibers with Long Range Order. *Nano Lett.* **2009**, *9*, 1678–1683. DOI: 10.1021/nl900265y.
108. Alizadeh-Osgouei, M.; Li, Y.; Vahid, A.; Ataee, A.; Wen, C. High Strength Porous PLA Gyroid Scaffolds Manufactured via Fused Deposition Modeling for Tissue-Engineering Applications. *Smart Mater. Med.* **2021**, *2*, 15–25. DOI: 10.1016/j.smaim.2020.10.003.
109. Abueidda, D. W.; Elhebeary, M.; Shiang, C.-S.; Pang, S.; Abu Al-Rub, R. K.; Jasiuk, I. M. Mechanical Properties of 3D Printed Polymeric Gyroid Cellular Structures: Experimental and Finite Element Study. *Mater. Des.* **2019**, *165*, 107597. DOI: 10.1016/j.matdes.2019.107597.
110. Bao, C.; Che, S.; Han, L. Discovery of Single Gyroid Structure in Self-Assembly of Block Copolymer with Inorganic Precursors. *J. Hazard. Mater.* **2021**, *402*, 123538. DOI: 10.1016/j.jhazmat.2020.123538.
111. Ma, M.; Rutledge, G. Nanostructured Electrospun Fibers. In *Polymer Science: A Comprehensive Reference*, **2012**; 7, pp 188–210.
112. Ma, M.; Thomas, E. L.; Rutledge, G. C.; Yu, B.; Li, B.; Jin, Q.; Ding, D.; Shi, A.-C. Gyroid-Forming Diblock Copolymers Confined in Cylindrical Geometry: A Case of Extreme

Makeover for Domain Morphology. *Macromolecules* **2010**, *43*, 3061–3071. DOI: 10.1021/ma9022586.
113. Kimizuka, N. Self-Assembly of Supramolecular Nanofibers. In *Self-Assembled Nanomaterials I: Nanofibers*; Shimizu, T. Ed., Springer: Berlin, Heidelberg, **2008**; *8*, pp 1–26.
114. Mishra, M. K.; Yu, H. L.; Molnar, J.; Baliga, V. Design of a Polymer Blend for One-Step Porous Fiber Fabrication. *Des. Monomers Polym.* **2009**, *12*, 273–278. DOI: 10.1163/156855509X436094.
115. McClements, D. J. Critical Review of Techniques and Methodologies for Characterization of Emulsion Stability. *Crit. Rev. Food Sci. Nutr.* **2007**, *47*, 611–649. DOI: 10.1080/10408390701289292.
116. Nikmaram, N.; Roohinejad, S.; Hashemi, S.; Koubaa, M.; Barba, F. J.; Abbaspourrad, A.; Greiner, R. Emulsion-Based Systems for Fabrication of Electrospun Nanofibers: Food, Pharmaceutical and Biomedical Applications. *RSC Adv.* **2017**, *7*, 28951–28964. DOI: 10.1039/C7RA00179G.
117. Hu, J.; Prabhakaran, M. P.; Ding, X.; Ramakrishna, S. Emulsion Electrospinning of Polycaprolactone: Influence of Surfactant Type towards the Scaffold Properties. *J. Biomater. Sci. Polym. Ed.* **2015**, *26*, 57–75. DOI: 10.1080/09205063.2014.982241.
118. Klier, J.; Tucker, C. J.; Kalantar, T. H.; Green, D. P. Properties and Applications of Microemulsions. *Adv. Mater.* **2000**, *12*, 1751–1757. DOI: 10.1002/1521-4095(200012)12:23<1751::AID-ADMA1751>3.0.CO;2-I.
119. He, Y.; Wu, F.; Sun, X.; Li, R.; Guo, Y.; Li, C.; Zhang, L.; Xing, F.; Wang, W.; Gao, J. Factors That Affect Pickering Emulsions Stabilized by Graphene Oxide. *ACS Appl. Mater. Interfaces.* **2013**, *5*, 4843–4855. DOI: 10.1021/am400582n.
120. Zhu, Y.; Murali, S.; Cai, W.; Li, X.; Suk, J. W.; Potts, J. R.; Ruoff, R. S. Graphene and Graphene Oxide: Synthesis, Properties, and Applications. *Adv. Mater.* **2010**, *22*, 3906–3924. DOI: 10.1002/adma.201001068.
121. Kim, J.; Cote, L. J.; Kim, F.; Yuan, W.; Shull, K. R.; Huang, J. Graphene Oxide Sheets at Interfaces. *J. Am. Chem. Soc.* **2010**, *132*, 8180–8186. DOI: 10.1021/ja102777p.
122. Gudarzi, M. M.; Sharif, F. Self Assembly of Graphene Oxide at the Liquid–Liquid Interface: A New Route to the Fabrication of Graphene Based Composites. *Soft Matter* **2011**, *7*, 3432–3440. DOI: 10.1039/c0sm01311k.
123. Memic, A.; Abudula, T.; Mohammed, H. S.; Joshi Navare, K.; Colombani, T.; Bencherif, S. A. Latest Progress in Electrospun Nanofibers for Wound Healing Applications. *ACS Appl. Bio Mater.* **2019**, *2*, 952–969. DOI: 10.1021/acsabm.8b00637.
124. Cheng, H.; Yang, X.; Che, X.; Yang, M.; Zhai, G. Biomedical Application and Controlled Drug Release of Electrospun Fibrous Materials. *Mater. Sci. Eng. C Mater. Biol. Appl.* **2018**, *90*, 750–763. DOI: 10.1016/j.msec.2018.05.007.
125. Li, Y.; Ko, F. K.; Hamad, W. Y. Effects of Emulsion Droplet Size on the Structure of Electrospun Ultrafine Biocomposite Fibers with Cellulose Nanocrystals. *Biomacromolecules* **2013**, *14*, 3801–3807. DOI: 10.1021/bm400540v.
126. Qi, H.; Hu, P.; Xu, J.; Wang, A. Encapsulation of Drug Reservoirs in Fibers by Emulsion Electrospinning: Morphology Characterization and Preliminary Release Assessment. *Biomacromolecules* **2006**, *7*, 2327–2330. DOI: 10.1021/bm060264z.
127. Tian, L.; Prabhakaran, M. P.; Ding, X.; Kai, D.; Ramakrishna, S. Emulsion Electrospun Vascular Endothelial Growth Factor Encapsulated Poly(L-Lactic Acid-co-ε-Caprolactone) Nanofibers for Sustained Release in Cardiac Tissue Engineering. *J. Mater. Sci.* **2012**, *47*, 3272–3281. DOI: 10.1007/s10853-011-6166-4.
128. Zhang, C.; Zhang, H. Formation and Stability of Core-Shell Nanofibers by Electrospinning of Gel-Like Corn Oil-in-Water Emulsions Stabilized by Gelatin. *J. Agric. Food Chem.* **2018**, *66*, 11681–11690. DOI: 10.1021/acs.jafc.8b04270.
129. Li, L.; Li, H.; Qian, Y.; Li, X.; Singh, G. K.; Zhong, L.; Liu, W.; Lv, Y.; Cai, K.; Yang, L. Electrospun Poly(ϵ-Caprolactone)/Silk Fibroin Core-Sheath Nanofibers and Their Potential Applications in Tissue Engineering and Drug Release. *Int. J. Biol. Macromol.* **2011**, *49*, 223–232.

130. Gu, X.; Song, X.; Shao, C. z.; Zeng, P. C.; Lu, X.; Shen, X.; Yang, Q. Electrospinning of Poly (Butylene-Carbonate) : Effect of Solvents on the Properties of the Nanofibers Film. *Int. J. Electrochem. Sci.* **2014**, *9*, 8045–8056.
131. Zhang, K.; Wang, H.; Huang, C.; Su, Y.; Mo, X.; Ikada, Y. Fabrication of Silk Fibroin Blended P(LLA-CL) Nanofibrous Scaffolds for Tissue Engineering. *J. Biomed. Mater. Res. A* **2010**, *93*, 984–993. DOI: 10.1002/jbm.a.32504.
132. Heydarkhan-Hagvall, S.; Schenke-Layland, K.; Dhanasopon, A. P.; Rofail, F.; Smith, H.; Wu, B. M.; Shemin, R.; Beygui, R. E.; MacLellan, W. R. Three-Dimensional Electrospun ECM-Based Hybrid Scaffolds for Cardiovascular Tissue Engineering. *Biomaterials* **2008**, *29*, 2907–2914. DOI: 10.1016/j.biomaterials.2008.03.034.
133. Camerlo, A.; Vebert-Nardin, C.; Rossi, R. M.; Popa, A. M. Fragrance Encapsulation in Polymeric Matrices by Emulsion Electrospinning. *Eur. Polym. J.* **2013**, *49*, 3806–3813. DOI: 10.1016/j.eurpolymj.2013.08.028.
134. Ma, L.; Shi, X.; Zhang, X.; Li, L. Electrospinning of Polycaprolacton/Chitosan Core-Shell Nanofibers by a Stable Emulsion System. *Colloids Surf. A* **2019**, *583*, 123956. DOI: 10.1016/j.colsurfa.2019.123956.
135. Wang, C.; Wang, M. Formation of Core-Shell Structures in Emulsion Electrospun Fibres: A Comparative Study. *Aust. J. Chem.* **2014**, *67*, 1403–1413. DOI: 10.1071/CH14214.
136. Sanders, E. H.; Kloefkorn, R.; Bowlin, G. L.; Simpson, D. G.; Wnek, G. E. Two-Phase Electrospinning from a Single Electrified Jet: Microencapsulation of Aqueous Reservoirs in Poly(Ethylene-Co-Vinyl Acetate) Fibers. *Macromolecules* **2003**, *36*, 3803–3805. DOI: 10.1021/ma021771l.
137. Mai, Y.; Eisenberg, A. Self-Assembly of Block Copolymers. *Chem. Soc. Rev.* **2012**, *41*, 5969–5985. DOI: 10.1039/c2cs35115c.
138. Tharmavaram, M.; Rawtani, D.; Pandey, G. Fabrication Routes for One-Dimensional Nanostructures via Block Copolymers. *Nano Converg.* **2017**, *4*, 12–12/13.
139. Hillmyer, M. A. Nanoporous Materials from Block Copolymer Precursors. *Adv. Polym. Sci.* **2005**, *190*, 137–181.
140. Wang, W.; Wang, W.; Li, H.; Lu, X.; Chen, J.; Kang, N.-G.; Zhang, Q.; Mays, J. Synthesis and Characterization of Graft Copolymers Poly(Isoprene-g-Styrene) of High Molecular Weight by a Combination of Anionic Polymerization and Emulsion Polymerization. *Ind. Eng. Chem. Res.* **2015**, *54*, 1292–1300. DOI: 10.1021/ie504457e.
141. Martin, T. B.; Jayaraman, A. Identifying the Ideal Characteristics of the Grafted Polymer Chain Length Distribution for Maximizing Dispersion of Polymer Grafted Nanoparticles in a Polymer Matrix. *Macromolecules* **2013**, *46*, 9144–9150. DOI: 10.1021/ma401763y.
142. Hadjichristidis, N.; Pitsikalis, M.; Iatrou, H.; Driva, P.; Chatzichristidi, M.; Sakellariou, G.; Lohse, D. Graft Copolymers. In *Encyclopedia of Polymer Science and Technology*, John Wiley & Sons, **2010**; pp 1–38.
143. Zhai, F.-Y.; Huang, W.; Wu, G.; Jing, X.-K.; Wang, M.-J.; Chen, S.-C.; Wang, Y.-Z.; Chin, I.-J.; Liu, Y. Nanofibers with Very Fine Core-Shell Morphology from Anisotropic Micelle of Amphiphilic Crystalline-Coil Block Copolymer. *ACS Nano.* **2013**, *7*, 4892–4901. DOI: 10.1021/nn401851w.
144. Wang, L.; Topham, P. D.; Mykhaylyk, O. O.; Yu, H.; Ryan, A. J.; Fairclough, J. P. A.; Bras, W. Self-Assembly-Driven Electrospinning: The Transition from Fibers to Intact Beaded Morphologies. *Macromol. Rapid Commun.* **2015**, *36*, 1437–1443.
145. Morkved, T. L.; Lu, M.; Urbas, A. M.; Ehrichs, E. E.; Jaeger, H. M.; Mansky, P.; Russell, T. P. Local Control of Microdomain Orientation in Diblock Copolymer Thin Films with Electric Fields. *Science* **1996**, *273*, 931–933. DOI: 10.1126/science.273.5277.931.
146. Zhou, Z.; Liu, T.; Khan, A. U.; Liu, G. Block Copolymer-Based Porous Carbon Fibers. *Sci. Adv.* **2019**, *5*, eaau6852/1–eaau6852/10. DOI: 10.1126/sciadv.aau6852.
147. Chen, S.-Y.; Huang, Y.; Tsiang, R. C.-C. Ozonolysis Efficiency of PS-b-PI Block Copolymers for Forming Nanoporous Polystyrene. *J. Polym. Sci. A Polym. Chem.* **2008**, *46*, 1964–1973. DOI: 10.1002/pola.22518.

148. Lee, J. S.; Hirao, A.; Nakahama, S. Polymerization of Monomers Containing Functional Silyl Groups. 5. Synthesis of New Porous Membranes with Functional Groups. *Macromolecules* **1988**, *21*, 274–276. DOI: 10.1021/ma00179a057.
149. Liu, G.; Ding, J.; Guo, A.; Herfort, M.; Bazett-Jones, D. Potential Skin Layers for Membranes with Tunable Nanochannels. *Macromolecules* **1997**, *30*, 1851–1853. DOI: 10.1021/ma961530b.
150. Hampu, N.; Bates, M. W.; Vidil, T.; Hillmyer, M. A. Bicontinuous Porous Nanomaterials from Block Polymers Radically Cured in the Disordered State for Size-Selective Membrane Applications. *ACS Appl. Nano Mater.* **2019**, *2*, 4567–4577. DOI: 10.1021/acsanm.9b00922.
151. Xu, H.; Xiao, H.; Ellison, C. J.; Mahanthappa, M. K. Flexible Nanoporous Materials by Matrix Removal from Cylinder-Forming Diblock Copolymers. *Nano Lett.* **2021**, *21*, 7587–7594. DOI: 10.1021/acs.nanolett.1c02097.
152. Potschke, P.; Paul, D. R. Formation of Co-Continuous Structures in Melt-Mixed Immiscible Polymer Blends. *J. Macromol. Sci. Polym. Rev.* **2003**, *C43*, 87–141.
153. Sánchez-Valdes, S.; Ramos-De Valle, L. F.; Manero, O. Polymer Blends. In *Handbook of Polymer Synthesis, Characterization, and Processing*; Saldívar-Guerra, E.; Vivaldo-Lima, E., Eds.; **2013**, pp 505–517.
154. Bognitzki, M.; Frese, T.; Steinhart, M.; Greiner, A.; Wendorff, J. H.; Schaper, A.; Hellwig, M. Preparation of Fibers with Nanoscaled Morphologies: Electrospinning of Polymer Blends. *Polym. Eng. Sci.* **2001**, *41*, 982–989. DOI: 10.1002/pen.10799.
155. Nayani, K.; Katepalli, H.; Sharma, C. S.; Sharma, A.; Patil, S.; Venkataraghavan, R. Electrospinning Combined with Nonsolvent-Induced Phase Separation to Fabricate Highly Porous and Hollow Submicrometer Polymer Fibers. *Ind. Eng. Chem. Res.* **2012**, *51*, 1761–1766. DOI: 10.1021/ie2009229.
156. Dayal, P.; Liu, J.; Kumar, S.; Kyu, T. Experimental and Theoretical Investigations of Porous Structure Formation in Electrospun Fibers. *Macromolecules* **2007**, *40*, 7689–7694. DOI: 10.1021/ma071418l.
157. Wei, M. K. B.; Sung, C.; Mead, J. Phase Morphology Control of the Electrospun Nanofibers from the Polymer Blends. *NSTI-Nanotech.* **2004**, *3*, 375–378.
158. Parreno, R. P., Jr.; Liu, Y.-L.; Beltran, A. B. A Sulfur Copolymers (SDIB)/ Polybenzoxazines (PBz) Polymer Blend for Electrospinning of Nanofibers. *Nanomaterials* **2019**, *9*, 1526. DOI: 10.3390/nano9111526.
159. Wang, Z.; Liu, X.; Macosko, C. W.; Bates, F. S. Nanofibers from Water-Extractable Melt-Blown Immiscible Polymer Blends. *Polymer* **2016**, *101*, 269–273. DOI: 10.1016/j.polymer.2016.08.058.
160. Xu, T.; Liang, Z.; Ding, B.; Feng, Q.; Fong, H. Polymer Blend Nanofibers Containing Polycaprolactone as Biocompatible and Biodegradable Binding Agent to Fabricate Electrospun Three-Dimensional Scaffolds/Structures. *Polymer* **2018**, *151*, 299–306. DOI: 10.1016/j.polymer.2018.07.074.
161. Nagamine, S.; Kosaka, K.; Tohyama, S.; Ohshima, M. Silica Nanofiber with Hierarchical Pore Structure Templated by a Polymer Blend Nanofiber and Surfactant Micelle. *Mater. Res. Bull.* **2014**, *50*, 108–112. DOI: 10.1016/j.materresbull.2013.10.025.
162. Jo, E.; Yeo, J.-G.; Kim, D. K.; Oh, J. S.; Hong, C. K. Preparation of Well-Controlled Porous Carbon Nanofiber Materials by Varying the Compatibility of Polymer Blends. *Polym. Int.* **2014**, *63*, 1471–1477. DOI: 10.1002/pi.4645.
163. Philip, P.; Tomlal Jose, E.; Chacko, J. K.; Philip, K. C.; Thomas, P. C. Preparation and Characterisation of Surface Roughened PMMA Electrospun Nanofibers from PEO – PMMA Polymer Blend Nanofibers. *Polym. Test* **2019**, *74*, 257–265. DOI: 10.1016/j.polymertesting.2019.01.009.
164. Kijeńska, E.; Prabhakaran, M. P.; Swieszkowski, W.; Kurzydlowski, K. J.; Ramakrishna, S. Interaction of Schwann Cells with Laminin Encapsulated PLCL Core-Shell Nanofibers for Nerve Tissue Engineering. *Eur. Polym. J.* **2014**, *50*, 30–38. DOI: 10.1016/j.eurpolymj.2013.10.021.
165. Sedghi, R.; Shaabani, A. Electrospun Biocompatible Core/Shell Polymer-Free Core Structure Nanofibers with Superior Antimicrobial Potency against Multi Drug Resistance Organisms. *Polymer* **2016**, *101*, 151–157. DOI: 10.1016/j.polymer.2016.08.060.